

MODES OF OPERATION, ANALYSIS AND PERFORMANCE OF THREE-PHASE CONVERTER-FED D. C. SEPERATELY EXCITED MOTOR

A Thesis Submitted
in Partial Fulfilment of the Requirements
for the Degree of
MASTER OF TECHNOLOGY

1981

By

RANA GHOSH

to the
DEPARTMENT OF ELECTRICAL ENGINEERING
INDIAN INSTITUTE OF TECHNOLOGY, KANPUR
AUGUST, 1981

1 JAN 1984

CEP ARY.

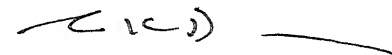
Acc No. 82642

EE-1901-M-GHO-MOD

CERTIFICATE

Certified that this work, "Modes of Operation, Analysis and Performance of Three-Phase Converter-fed D.C. Separately Excited Motor" by Rana Ghosh is carried out under my supervision and is not submitted elsewhere for a degree.

Kanpur
July 1981.



Dr. G.K. Dubey
Professor

Department of Electrical Engineering
INDIAN INSTITUTE OF TECHNOLOGY, KANPUR

ACKNOWLEDGEMENTS

I wish to express my deep sense of gratitude to Dr. G.K. Dubey for his able and dynamic guidance. I wish to thank Dr. A. Joshi and Mr. P.S. Bhat for useful discussions with them. I wish to thank Mr. P.D. Parikh, Mr. B.D. Sharma, Mr. H.K. Patel, Mr. A. Kellogg, Mr. E.S.N. Prasad and all my friends for their help at various stages. I am grateful to Mr. Gorpade and Mr. O.P. Arora for their cooperation.

I am also thankful to Mr. H.K. Nathani for his excellent typing.

Kanpur
July 1981

- Rana Ghosh

CONTENTS

	Page
CHAPTER I 1. INTRODUCTION	1
1.1 MODE IDENTIFICATION	1
1.2 ANALYSIS AND PERFORMANCE	2
1.3 CHOICE OF FILTER INDUCTANCE	2
CHAPTER II LITERATURE SURVEY ON STEADY- STATE ANALYSIS AND PERFORMANCE OF CONVERTER-FED DC SEPERATELY EXCITED MOTOR	5
CHAPTER III MODE IDENTIFICATION, ANALYSIS AND PERFORMANCE OF THREE PHASE CONVERTER-FED DRIVES	15
3.1 MODE IDENTIFICATION	15
3.2 PERFORMANCE EQUATIONS	23
3.3 BOUNDARY BETWEEN CONTINUOUS AND DISCONTINUOUS CONDUCTION	34
3.4 METHOD OF MODE SELECTION	37
3.5 PERFORMANCE COMPUTATIONS	41
3.6 CHOICE OF FILTER INDUCTANCE	45
CHAPTER IV EXPERIMENTAL INVESTIGATION	48
4.1 THE FIRING CIRCUIT	48
4.2 EXPERIMENTAL VERIFICATION	50
CONCLUSIONS	
REFERENCES	
APPENDIX	

NOMENCLATURE

E_m	: Peak value of a.c. input voltage, V.
E_d	: Motor back emf, V.
i_a	: Instantaneous armature current, Amp.
i_n	: Instantaneous armature current in p.u.
ωN	: Speed in p.u.
T_N	: Torque in p.u.
L_a	: Total inductance in armature circuit, H
R_a	: Armature resistance, ohms
RF	: Ripple factor
PF	: Power factor
DF	: Distortion factor
α	: Triggering angle
β	: Extinction angle
γ	: Angle at which instantaneous a.c. supply voltage is equal to back emf of motor
ϕ	: $\tan^{-1}(\omega L_a/R_a)$ in radians
ω	: Angular frequency of a.c. supply voltage, rad/sec.
$I_{av}(\alpha)$: Average current in p.u.
i_{sn}	: Instantaneous source current in p.u.
VR	: Voltage ratio
PHI	: same as ϕ

ABSTRACT

No work has been reported on the mode identification of three-phase converter fed d.c. seperately excited motor and so accurate analysis was not possible. In this thesis the modes of operation have been identified and the drive has been analysed. The speed-torque characteristic and the armature current ripple have been computed. These results can be directly used for any motor as they have been plotted with normalised variables. The power-factor, distortion-factor and different harmonic contents in the source current have also been computed. These have been found for a particular motor, but the same approach can be extended for any motor.

A method for the calculation of filter inductance is presented, which eliminates discontinuous conduction and keeps the ripple within permissible limits.

CHAPTER I

INTRODUCTION

Converter-fed dc drives find wide application in the industry. For small drives the single phase converter is used and for medium and large drives the three-phase converter is used. The present thesis deals with the mode identification and accurate analysis of the three-phase converter-fed dc separately excited motor.

1.1 MODE IDENTIFICATION

The converter-fed dc separately excited motor could experience discontinuous conduction at light loads and high speeds. Mehta and Mukhopadhyay [1] have described various modes of operation of single-phase converter-fed dc separately excited motor. Subbaiah and Palanichamy [2] have described an additional mode of operation ^{under} regeneration. However, various modes of operation of three-phase converter fed dc drive have not been identified and therefore accurate methods of analysis are not available.

In this thesis the various modes of operation have been identified for three-phase full and half controlled converter-fed dc separately excited motor. The description of the various modes of operation for three-phase converter-fed drives is given in Chapter III.

1.2 ANALYSIS AND PERFORMANCE

With the help of the various modes of operation which have been identified, the drive has been analysed over the full operating region. The performance equation pertaining to the different modes of operation have been derived. With the help of these equations the speed-torque characteristic has been derived analytically for the dc separately excited motor and the maximum ripple factor has been found for the armature current. The power-factor, distortion factor and the harmonic contents have been found for the source current. The speed-torque and the maximum ripple factor curves have been plotted on normalised axes so that they can be used to get the speed torque variation and the maximum ripple factor for any dc separately excited motor. The power-factor, distortion factor and the harmonic contents in the source current have been found for a particular motor and ^{load} phase-angle. The same approach can be easily extended for any other ^{load} phase angle value.

The various performance curves have been shown in Chapter III.

1.3 CHOICE OF FILTER INDUCTANCE

For a converter-fed dc drive, the armature current could be continuous or discontinuous. This current is not constant but has an ac ripple superimposed on a dc

value. The ac ripple and discontinuous conduction increase the motor burden and losses, leading to derating of the motor and reducing its efficiency. Also under discontinuous conduction the motor speed regulation is poor. So efforts have to be made to eliminate discontinuous conduction and decrease the ripple content.

Discontinuous conduction can be eliminated and ripple in armature current can be reduced either by increasing the pulse number or by introducing a filter inductance. Increasing the pulse number increases the cost manifold. Increase in armature circuit inductance is not always desirable because addition of external inductance reduces the efficiency, increases the cost, weight, size and noise and deteriorates the transient response of the motor.

If an external inductance is absolutely necessary, its value should be just sufficient to eliminate discontinuous conduction and keep the ac ripple within permissible limits. This will ensure that the adverse effects mentioned above are minimal.

Mehta and Mukhopadhyay [1] have described a method for calculating the minimum inductance to avoid discontinuous conduction for a single phase converter-fed dc drive. Their method suffers from the disadvantages that the armature resistance is neglected and the nature of the load speed-torque variation

is not taken into account. Subbaiah and Palanichamy [3] have extended this work to take into account the armature resistance but here again the load speed torque variation is not taken into account. G.K. Dubey [4] has described a method for calculating the critical value of filter inductance for a dc separately excited motor fed by chopper. This method has been extended by Anjenyulu [5] for the single-phase converter-fed dc separately excited motor. In this thesis this method for the calculation of optimum value of inductance has been further extended for the three-phase converter-fed drive, which takes into account the nature of load speed-torque characteristics. Programs have been given in terms of normalised variables. These can be used to obtain an optimum value of filter inductance for any three-phase converter-fed dc separately excited motor.

The various modes of operation and the different performance curves have been verified experimentally for fully controlled operation.

CHAPTER II

LITERATURE SURVEY ON STEADY-STATE ANALYSIS AND PERFORMANCE OF CONVERTER-FED DC SEPERATELY EXCITED MOTOR

In thyristor controlled converter-fed dc drives, the armature current has superimposed harmonic ripple. For a dc separately excited motor, with low armature inductance, discontinuous conduction could occur under light load conditions. Thus broadly the modes of conduction can be classified to be either continuous or discontinuous.

It was generally believed that in a converter, the thyristors could not be triggered before the input voltage is greater than the back emf of the motor. However, Mehta and Mukhopadhyay [1] have shown that if armature current is present, the back emf does not appear across the thyristors to reverse bias them. Thus if armature current is present, the thyristors could be triggered at any α greater than 0. With this basic idea, they have redefined the modes of operation of single phase converter-fed dc drives, which are described below.

Fig. 2.1 shows a single phase converter feeding a separately excited motor. With the free-wheeling diode in circuit, it will be capable of one-quadrant operation. It must be noted that in the absence of armature current, the back emf of the motor appears across the converter

output terminals and the performance of the motor depends upon the mode of operation. The different modes of operation are:

Mode 1 (Fig. 2.2(a)): In this mode the current is discontinuous and the earliest instant at which the thyristors could be triggered is when the input voltage is equal to the back emf.

Mode 2 (Fig. 2.2(b)): In this mode also the current is discontinuous but the extinction angle β lies between α and γ . Since at α , armature current is present, the back emf of the motor does not appear across the thyristors, which take over conduction even when the input voltage is less than the back emf. From β to γ discontinuous conduction occurs and assuming long gate pulses the thyristors start conducting again from γ and remains in conduction until $(\alpha + \pi)$ when the next thyristors are triggered.

Mode 3 (Fig. 2.2(c)): In this mode the current is continuous with α being greater than γ .

Mode 4 (Fig. 2.2(d)): In this mode the current is continuous with α being less than γ . As armature current is always present the thyristors would take over conduction when triggered.

These modes hold good for a converter-fed dc drive under motoring conditions only. This work has been further extended to the regenerative region by Subbiah and Palanichamy [2]. They have identified a mode which is described below. It is assumed that the thyristors gates are given pulses of π radians duration.

Mode 5 (Fig. 2.2(e)): This mode was known even earlier for regeneration with $\alpha < (\pi - \gamma)$. This current is present from α to β only.

Mode 6 (Fig. 2.2(f)): In this mode discontinuous conduction occurs with α greater than $(\pi - \gamma)$. Here the gated thyristors would conduct upto β , when the current falls to zero. The zero current interval would continue till $(2\pi - \gamma)$ after which the same thyristors would again take over conduction till at $(\pi + \gamma)$ the next thyristors are triggered.

Modes 1 to 4 hold good for full and half controlled converter-fed dc drives, whereas Modes 5 and 6 are valid for fully controlled converter.

With these new modes taken into account the operating diagram put forward by Dewan and Straughen [6] have been modified by the authors. ^[1,2] The new operating diagram is shown in Fig. 2.3(a). The region PQRTF has been modified with modes 2 and 4 and the region ~~WKGFEH~~ ^{WKGFEH} has been modified with mode 6.

In the operating diagram (Fig. 2.3(a)) the different modes are represented by the following regions. For an example we shall take ϕ (the load phase angle) to be 60° . 'm' is the ratio of the back emf to the peak input voltage.

Region PQEFGJRM represents discontinuous conduction

Region MRJGFHITM represents continuous conduction.

- (1) Region RQEJR represents mode 1
- (2) Region PQRM represents Mode 2 along with the mode of conduction where $\alpha < \gamma$ and conduction starts at γ .
- (3) Region TRJT represents Mode 3
- (4) Region MRTM represents Mode 4
- (5) Region JEGJ represents Mode 5
- (6) Region GEFG represents Mode 6
- (7) Region TJGFHIT represents continuous conduction under regeneration.

Discontinuous conduction in the motor operation makes the steady state and transient response poor. Moreover the speed regulation is poor and commutation burden is increased. Due to this the motor has to be derated. To avoid discontinuous conduction in the armature current a reactor is usually inserted in the armature circuit. The choice of the reactor is an important factor and has to be such that it will avoid

discontinuous conduction and also will not adversely affect the transient response. Moreover large inductance would mean more cost, weight and losses.

Mehta and Mukhopadhyay have put forward a method for the calculation of minimum inductance for continuous conduction in single phase converter fed d.c. drive. The method put forward by them incorporates all the modes of operation identified by them and is described below. In calculation of the inductance value the armature resistance is neglected.

The generalised voltage equation for the system shown in Fig. 21 is:

$$bE_m \sin wt = L_a \frac{di_a}{dt} + R_a i_a + E_d \quad (1)$$

b is 0, 1 or -1 depending upon instantaneous circuit condition.

Case I: $\alpha \leq \gamma$

(a) For one-quadrant drive the conditions for the generalised equation are:

$$b = 1 \quad \gamma \leq wt \leq \pi$$

$$b = 0 \quad \pi \leq wt \leq (\pi + \alpha)$$

$$b = -1 \quad \pi + \alpha \leq wt \leq (\pi + \gamma)$$

Solving Equation 1 with the above conditions and neglecting R_a we have

$$I_d = \frac{E_m}{\pi \omega L} \left[\pi \cos \gamma + \gamma + (\gamma - \alpha) \cos \alpha + \sin \alpha \right] - \frac{\pi E_d}{2 \omega L} \quad (2)$$

also for continuous conduction:

$$E_d = \frac{E_m}{\pi} (1 + \cos \alpha) \quad (3)$$

Substituting (3) in (2) and after rearranging the terms we get

$$L = K \left[2\pi \cos \gamma + 2\gamma + 2 \sin \alpha - \pi - (\pi + 2\alpha - 2\gamma) \cos \alpha \right] \quad (4)$$

where $K = \text{inductance constant} = E_m / 2\pi \omega I_d$

(b) For two-quadrant drive we have

$$b = 1 \quad \gamma \leq \omega t \leq \pi + \alpha$$

$$b = -1 \quad \pi + \alpha \leq \omega t \leq \pi + \gamma$$

Solving Equation (1) with these conditions we get

$$I_d = \frac{E_m}{\pi \omega L} \left[\pi \cos \gamma + 2 \sin \alpha + 2(\gamma - \alpha) \cos \alpha \right] - \frac{E_d}{2 \pi \omega L} \pi^2 \quad (5)$$

and for continuous conduction we have

$$E_d = \frac{E_m}{\pi} \cos \alpha \quad (6)$$

Substituting (6) in (5) we get

$$L = 2K \left[\pi \cos \gamma + 2 \sin \alpha + (2\gamma - 2\alpha - \pi) \cos \alpha \right] \quad (7)$$

Case II $\alpha > \gamma$

(a) For one-quadrant drive

$$b = 1 \quad \alpha \leq \omega t \leq \pi$$

$$b = 0 \quad \pi \leq \omega t \leq (\pi + \alpha)$$

out

by carrying out the above operations we get

$$L = K[2\alpha + 2 \sin \alpha + \pi \cos \alpha - \pi] \quad (8)$$

(b) For two quadrant drive

$$b = 1 \quad \alpha \leq \omega t \leq \pi + \alpha$$

Solving (1) and after the necessary operations we get

$$L = 4K \sin \alpha \quad (9)$$

Subbiah and Palanichamy [3] have extended this method to the regeneration case incorporating the new modes identified by them. The minimum inductance required (in terms of K) as a function of triggering angle is plotted in Fig. 2.3(b). With this plot we can find the inductance for a particular firing angle and a given average armature current. They have also suggested another method in which the armature circuit resistance is taken into account. A graphical approach is taken, as analytical solution is tedious. They have used the modified operating diagram shown in Fig. 2.3(a). This method is described here.

Let us consider the load phase angle to be $\phi = 60^\circ$. For the trigger angle indicated by point x in Fig. 2.3(a), the ordinate XY is the normalised back emf at the limit of continuous conduction and XZ gives the normalised output voltage of the converter. Thus YZ gives the $I_d R_a$ drop at the limit of continuous conduction. The $I_d R_a$ drop is plotted against the firing angle α for different values of ϕ as shown in Fig. 2.3(c). Here also knowing the average output current and the firing angle, the minimum ϕ can be chosen. Knowing the armature resistance and inductance, the extra filter inductance can be calculated. In both the methods the nature of the load speed-torque characteristic is not taken into account.

G.K. Dubey[4] has described a method by which the filter inductance can be calculated for a chopper-fed dc drive. The inductance value chosen, is just sufficient to eliminate discontinuous conduction and keeps the ac ripple within permissible limits. In this method the load nature of the speed-torque characteristic is taken into account, so that we get the minimum inductance value over the whole operating range of the drive. This will ensure that the losses in inductance, increase in cost, weight, size and noise will be minimal. There will also be minimal deterioration in the transient response.

Anjenyulu [5] has extended this approach for the single phase converter fed dc drive. His method has the advantages listed above. Taking into account the different modes of operation, the performance equation is derived for each mode. Under critical conditions we have for:

Case A: $\alpha < \gamma$

$$i(\omega t) \Big|_{\omega t = \gamma} = 0 \quad \text{as the initial condition}$$

$$\text{and } i(\omega t) \Big|_{\omega t = \pi + \gamma} = 0 \quad \text{as the final condition}$$

Incorporating these conditions along with appropriate values of b for different operating conditions in Equation (1) a solution is obtained under critical condition, i.e., the boundary between continuous and discontinuous conduction.

Case B: $\alpha > \gamma$

$$i(\omega t) \Big|_{\omega t = \alpha} = 0 \quad \text{as the initial condition}$$

$$\text{and } i(\omega t) \Big|_{\omega t = \pi + \alpha} = 0 \quad \text{as the final condition}$$

Again with these conditions, expressions are derived under critical conditions. With the help of these expressions, various boundary curves are plotted on a normalised speed-torque plane for different value of ϕ .

The minimum speed torque curve of the motor is also plotted and the value of ϕ which will avoid discontinuous conduction is found. For this value of ϕ the ripple

factor is found." If the ripple factor is within permissible limits then we choose this value of δ otherwise we go in for a higher value. Knowing the armature resistance and inductance the extra filter inductance value can be calculated."

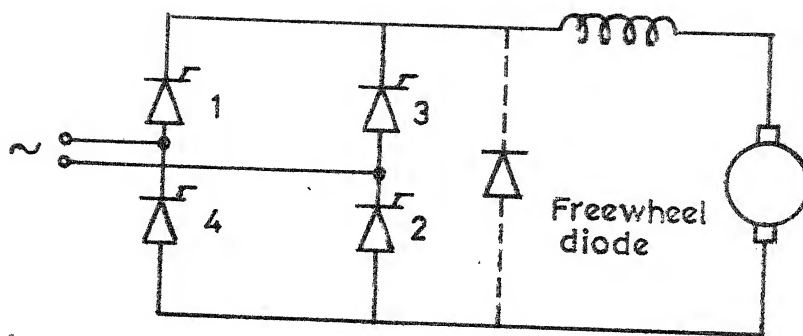


FIG.2.1

single - phase converter - fed
d.c. seperately excited motor.

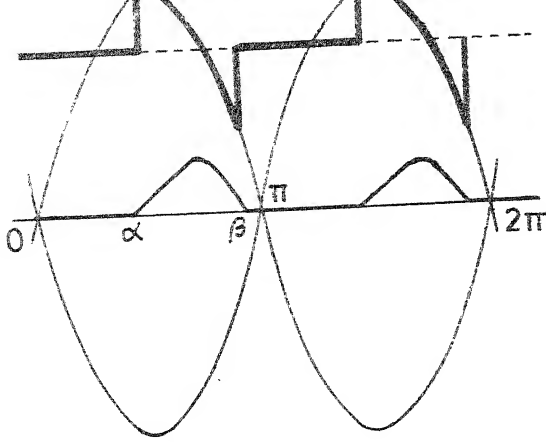


Fig. 2.2 (a)

Mode 1
discontinuous
conduction with
 $\alpha > \gamma$

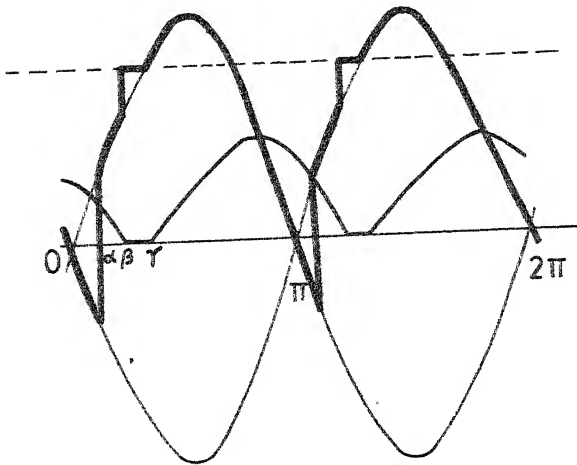


Fig. 2.2 (b)

Mode 2
discontinuous
conduction with
 $\alpha < \gamma$

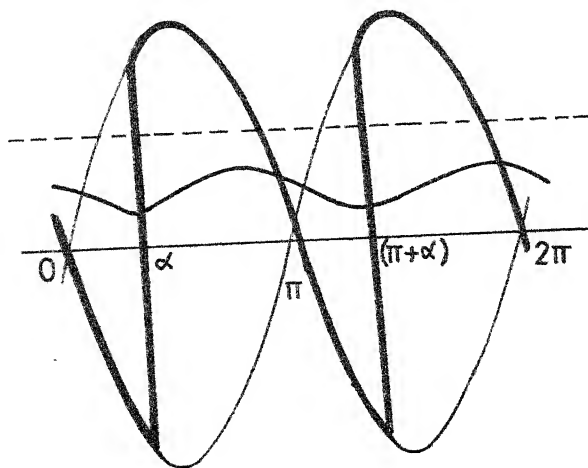


Fig. 2.2 (c)

Mode 3
continuous
conduction
with $\alpha > \gamma$

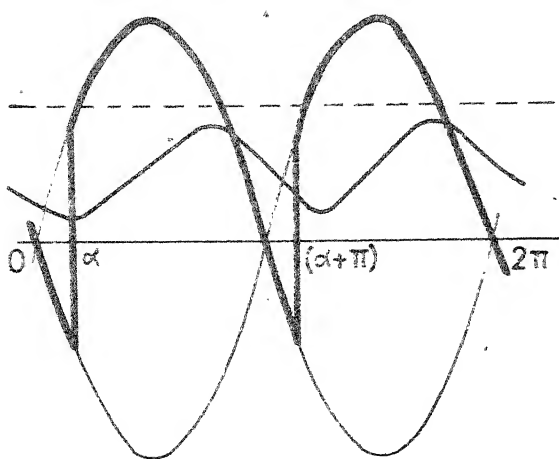


Fig. 2.2(d)

Mode 4
~~continuous~~ continuous
 conduction with
 $\alpha < r$

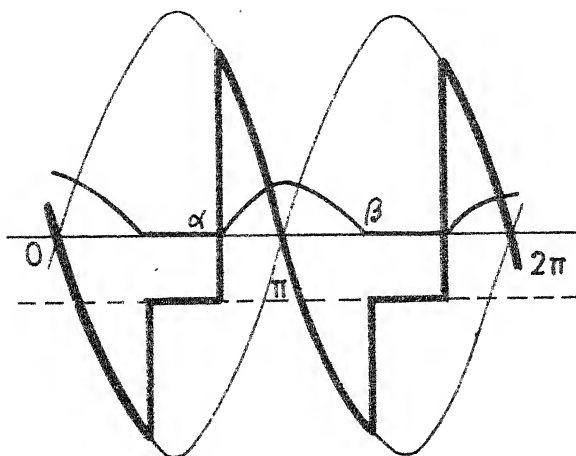


Fig. 2.2 (e)

Mode 5
 discontinuous
 conduction
 with $\alpha < (\pi - r)$

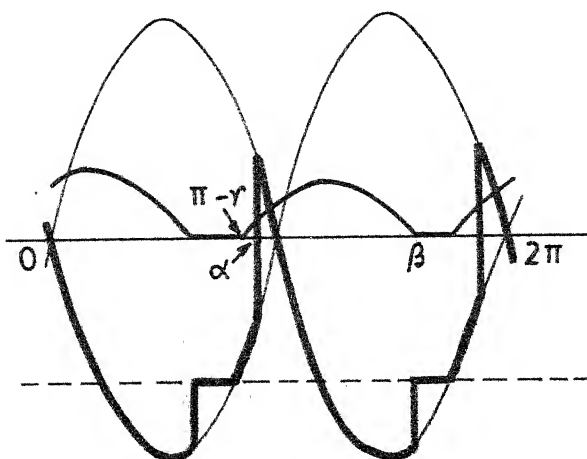


Fig. 2 2 (f)

Mode 6
 discontinuous
 conduction
 with $\alpha > (\pi - r)$

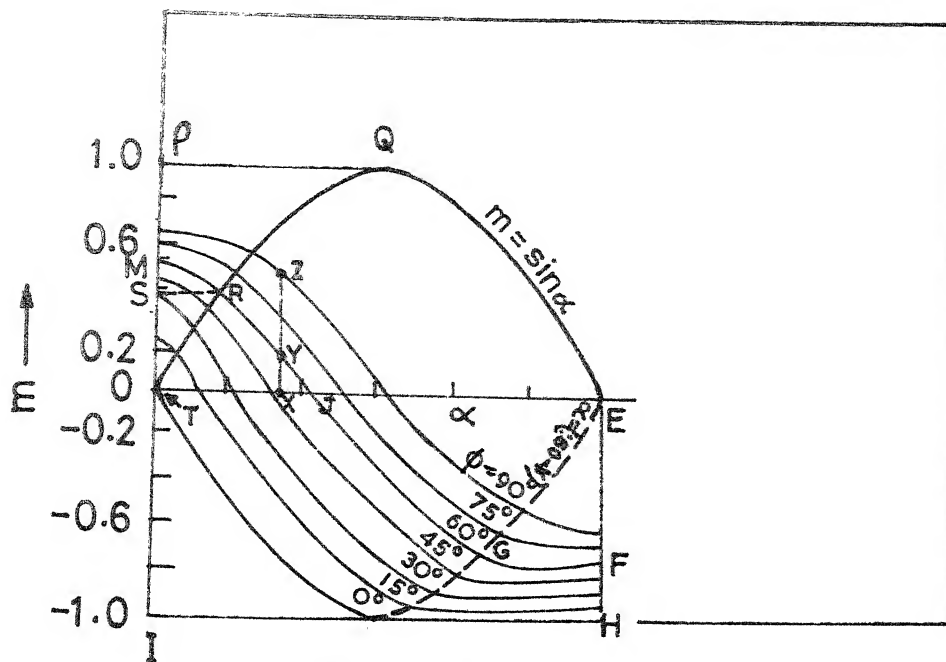


FIG. 2.3(a)

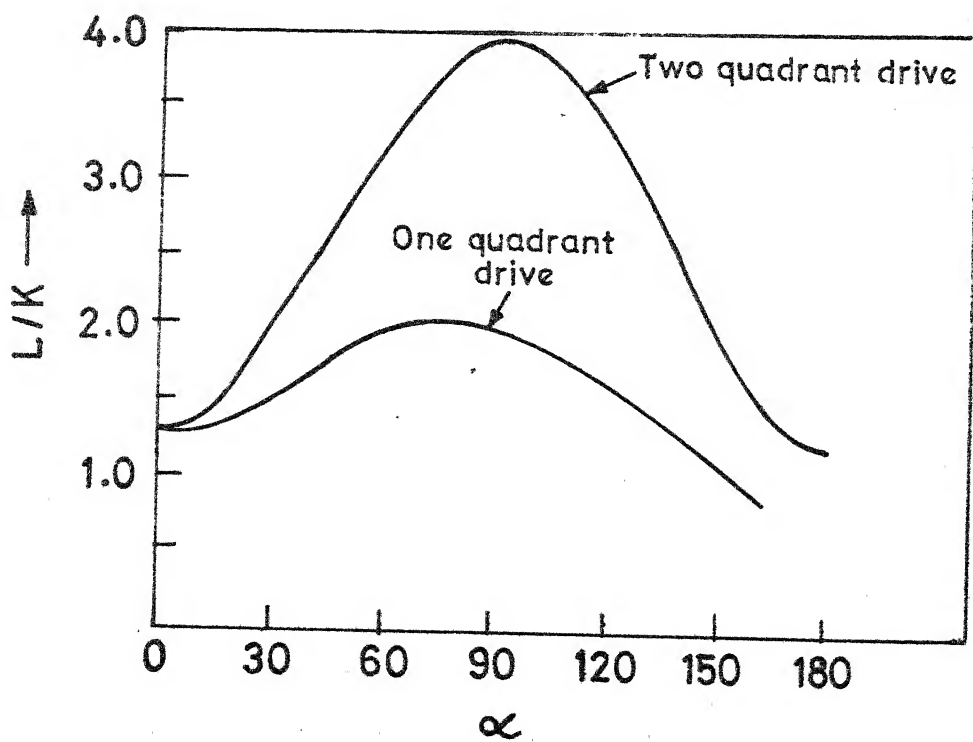


FIG. 2.3(b)

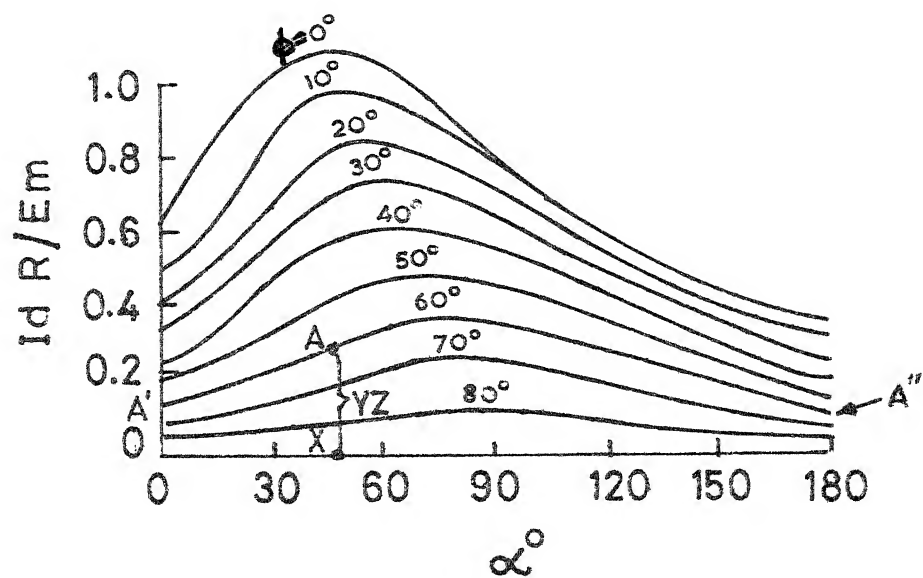


FIG. 2.3 (c)

CHAPTER III

MODE IDENTIFICATION, ANALYSIS AND PERFORMANCE OF THREE PHASE CONVERTER-FED DRIVES

3.1 MODE IDENTIFICATION

3.1 (a) Half Controlled Operation

Mode 1: (Figures 3.2(a), 3.2(b) and 3.2(c)) Continuous Conduction:

In this mode the current is continuous and the thyristors can be triggered at any angle as the back emf will not appear as a reverse bias across the thyristors.

In Fig. 3.2(a) the thyristors are triggered at an angle less than the angle at which the instantaneous input voltage is equal to the motor back emf (i.e. γ). When a thyristor T1 is triggered at $(\alpha + \pi/3)$, it takes over conduction from T5 and the devices which conduct are T1 and D6. As the input voltage is less than the back emf, the current decreases till a little after $(\gamma + \pi/3)$ (the current decreases till the $i_a R_a$ drop plus the back emf become equal to the input voltage). Thereafter the current increases till a little before $(2\pi/3 - \gamma)$ as the input voltage is greater than the back emf. After this instant the current decreases till at $2\pi/3$ diode D2 takes over conduction from D6 and the devices which conduct are T1 and D2. The current further decreases till a little after $(2\pi/3 + \gamma)$, increases henceforth till a

little before $(\pi - \gamma)$, then decreases again till at $(\pi + \gamma)$ the next thyristor i.e., T3 is triggered, which then takes over conduction from T1 and the cycle repeats.

In Fig. 3.2(b), the thyristors are triggered at an angle greater than γ , but less than $\pi/3$. Due to this no free wheeling takes place. When at $(\alpha + \pi/3)$ thyristor T1 is triggered it takes over conduction from T5 and the devices which conduct are T1 and D6. As the input voltage is greater than the back emf, the current increases till at $2\pi/3$, diode D2 takes over conduction from D6. The devices which conduct are T1 and D2. As the input voltage is still greater than the back emf, the current further increases till a little before the input voltage equals the back emf. The current henceforth decreases till at $(\alpha + \pi)$ the thyristor T3 takes over conduction and the cycle repeats.

In Fig. 3.2(c), the firing angle is greater than $\pi/3$ and free wheeling takes place after $wt = 4\pi/3$. When at $wt = (\alpha + \pi/3)$ T1 is triggered, it takes over conduction from T5. The devices which conduct are T1 and D2. The current rises till about $(4\pi/3 - \gamma)$ and starts decreasing thereafter. At $wt = 4\pi/3$, diode D4 takes over conduction from D2 and free-wheeling starts. The free-wheeling period prevails till the next thyristor T3 is triggered at $wt = (\alpha + \pi)$.

Mode 2: (Figures 3.2(d), 3.2(e))

Discontinuous conduction with $\alpha < \gamma$.

In this mode, current reaches zero value between α and γ . At $\omega t = \alpha + \pi/3$, when T1 is triggered, it takes over conduction from T5 as armature current is present in the ~~circuit~~ ^{circuit}. But as the input voltage is less than the back emf the current decreases till it reaches a zero value. The zero current interval prevails till $\omega t = \gamma + \pi/3$ where due to presence of long pulses T1 starts conducting again along with D6. The current increases till about $\omega t = (2\pi/3 - \gamma)$. The current decreases thereafter and at $\omega t = 2\pi/3$, diode D2 takes over conduction from D6. The current still decreases till $\omega t = (\gamma + 2\pi/3)$. The current then increases till about $\omega t = (\pi - \gamma)$, decreases thereafter till at $(\alpha + \pi)$ when T3 is triggered to take over conduction from T1 and the cycle repeats.

Mode 3: (Fig. 3.2(f)) Discontinuous conduction with

$$\gamma < \alpha < \pi/3$$

In this mode, discontinuous conduction occurs with α less than $\pi/3$ but greater than γ . At $\omega t = \alpha + \pi/3$, if T1 is triggered it starts conducting along with diode D6. The current increases till $\omega t = 2\pi/3$ where D2 takes over conduction. If $\gamma > 0$ the current rises till about $\pi - \gamma$, and decreases till $\omega t = 2\pi/3$, where D2 takes over conduction from D6. The current increases or decreases from this

instant onwards depending upon whether the input voltage is greater than or less than the back emf. If $\gamma > 0$ the current decreases till about $\omega t = (\gamma + 2\pi/3)$ and increases thereafter till $\omega t = (4\pi/3 - \gamma)$. If however, $\gamma < 0$ the current further increases from $\omega t = 2\pi/3$ till about $\omega t = (\pi - \gamma)$. The current thereafter decreases and reaches zero value and the devices stop conducting. The zero current interval prevails till $\omega t = \alpha + \pi$ where T3 is triggered and the cycle repeats. No free-wheeling occurs as the firing angle is less than $\pi/3$.

Mode 4: Fig. 3.2(g), Discontinuous conduction with $\gamma < \alpha < \pi/3$

In this mode the current goes to zero twice between successive firing of thyristors. At $\omega t = (\alpha + \pi/3)$, T1 is gated. As the input voltage is greater than the back emf, T1 starts to conduct along with D6. The current increases till about $(2\pi/3 - \gamma)$, after which the current decreases and falls to zero value. Zero current interval prevails till $(\gamma + \pi/3)$, after which due to the presence of gating pulses at T1, it starts conducting along with D2. The current increases till about $(\pi - \gamma)$ and decreases henceforth till it reaches zero current value and the devices stop conducting. This conduction prevails till $(\alpha + \pi)$, where T3 is triggered and the cycle repeats.

Mode 5: (Fig. 3.2(h)) Discontinuous Conduction

with $\gamma < \alpha < \pi/3$

In this mode the current again goes to zero twice between two successive firing of thyristors. At $\omega t = (\alpha + \pi/3)$, T1 is triggered which starts to conduct alongwith D6. The current rises till $\omega t = (2\pi/3 - \gamma)$ after which it decreases till at $\omega t = 2\pi/3$, diode D2 takes over conduction. As the input voltage is still less than the back emf the current further decreases and reaches zero value where the devices stop conducting. This zero current interval remains till $\omega t = (\gamma + 2\pi/3)$, where due to the presence of gate pulses at T1, it starts conducting again along with diode D2. The current increases till about $\omega t = (\pi - \gamma)$. The current then decreases again and reaches zero value. The zero current interval prevails till $\omega t = \alpha + \pi$, when thyristor T3 is triggered.

Mode 6: (Fig. 3.2(i)) Discontinuous Conduction with

$$(\pi/3 - \gamma) \leq \alpha \leq (\gamma + \pi/3)$$

This mode is similar to Mode 3. If α is greater than $(\pi/3 - \gamma)$ and less than $(\gamma + \pi/3)$ and if no current is present at the instant of triggering, the devices do not conduct immediately. Due to the presence of long pulses, conduction starts at $\omega t = (\gamma + 2\pi/3)$. The current increases from this instant onwards till $\omega t = (2\pi/3 - \gamma)$ and then decreases till it reaches zero value and the devices stop

conducting the zero current interval in this mode would prevail till $\omega t = (4\pi/3 + \gamma)$ where the next set of devices take over."

Mode 7: Fig. 3.2(j) Discontinuous conduction with $\alpha > \pi/3$ but $\beta < \pi$

In this mode the firing angle α is greater than $\pi/3$ but as the armature current reaches zero value before free-wheeling action can take place, this mode is similar to mode 3. At $\omega t = (\alpha + \pi/3)$ thyristor T1 is triggered which starts conducting along with diode D2. The current rises till $\omega t = (\pi - \gamma)$ and thereafter decreases till zero value is reached. In this mode angle β at which current falls to zero value is less than π . At $\omega t = (\alpha + \pi)$ thyristor T3 is triggered and the cycle repeats."

Mode 8: Fig. 3.2(k) Discontinuous conduction with $\alpha > \pi/3$ and $\beta > \pi$

In this mode discontinuous conduction takes place with $\alpha > \pi/3$. At $\omega t = \alpha + \pi/3$, thyristor T1 is triggered. It starts to conduct along with diode D2. As the input voltage is greater than the back emf, the current rises till about $\omega t = (\pi - \gamma)$ after which it decreases till at $\omega t = 4\pi/3$ when diode D4 takes over conduction from D2. Due to the simultaneous conduction of devices T1 and D4, free-wheeling action occurs. This is to say the current circulates within a loop formed by these devices and the motor. This current

gradually decays and zero current is reached where the devices stop conducting. The zero current interval prevails till $\omega t = (\alpha + \pi)$ where thyristor T3 is triggered and the cycle repeats.

3.1 (b) Fully Controlled Operation

Mode 1: Fig. 3.3(a) Continuous Conduction

In this mode the current is continuous and as the back emf does not appear as a reverse bias across the thyristors, they can be triggered at any instant. At $\omega t = (\alpha + \pi/3)$, T1 is gated and it takes over conduction from T5. The devices which conduct are T1 and T6. If α is greater than γ , the current rises till a little before $(2\pi/3 - \gamma)$ and decreases henceforth till at $\omega t = \alpha + 2\pi/3$, T2 is gated and it takes over conduction from T6. The devices which conduct are T1 and T2 and the cycle repeats.

If α is less than γ , when T1 is triggered, it takes over conduction from T5, but since the input voltage is less than the back emf the current continues to decrease till a little after $\omega t = \gamma + \pi/3$. The current increases thereafter till the input voltage is greater than the back emf of the motor, decreases henceforth till at $\omega t = \alpha + 2\pi/3$, when thyristor T2 is gated, which takes over conduction from T6 and the cycle repeats.

Mode 2: Fig. 3.3(b), 3.3(c) Discontinuous conduction with $\alpha < \gamma$

In this mode, the current is discontinuous, but the extinction angle lies between α and γ . Since armature current is present at the instant of triggering, the fired thyristor will take over conduction. If thyristor T1 is triggered at $\alpha + \pi/3$, it takes over conduction from T5. As the input voltage is less than the back emf, the current decreases and reaches zero value. The zero current interval prevails till $\omega t = \gamma + \pi/3$ where due to long pulses present the same set of thyristors T1 and T2 start conducting again. The current rises from zero value, reaches a maximum at about $\omega t = 2\pi/3 - \gamma$, and start decreasing thereafter till at $\alpha + 2\pi/3$ when T2 is triggered and takes over conduction from T6. The cycle repeats.

Mode 3: Fig. 3.3(d) Discontinuous conduction with $\alpha > \gamma$

In this mode, the earliest instant at which the thyristor T1 can be triggered is at $\omega t = \gamma + \pi/3$. With $\alpha > \gamma$, when T1 is fired at $\omega t = \alpha + \pi/3$, it will take over conduction along with T6 which was also receiving gate pulses. This is so because the input voltage is greater than the back emf at the instant of firing the thyristors. The current rises till about $\omega t = 2\pi/3 - \gamma$, decreases henceforth till it reaches a zero value and the thyristors are cut off. The zero current interval prevails till at $\omega t = \alpha + 2\pi/3$ when T2 is triggered

and since T1 is already getting gate pulses at this instant, T1 and T2 conduct.

3.2 PERFORMANCE EQUATIONS

It is assumed that

- (a) the thyristors and diodes are ideal switches
- (b) the resistances and inductance of the motor armature are constant
- (c) the commutation overlap due to source inductance is negligible
- (d) during the given steady state condition, the motor speed is constant.
- (e) the gate pulses are of $2\pi/3$ radians duration.

Fig. 3.1 shows the basic circuit for the three phase converter controlled, separately excited d.c. motor. The performance equations under different operating conditions are given below.

3.2(a) Fully Controlled Operation

Mode 1: (Fig. 3.3(a)) Continuous Conduction

The equation governing the system operation is:

$$L_a \frac{di_a}{dt} + R_a i_a + E_d = E_m \sin wt \quad (\alpha + \pi/3) \leq wt \leq (\alpha + 2\pi/3) \quad (3.1)$$

solving (3.1) with the condition that

$$i_a(wt) \Big|_{wt = \alpha + \pi/3} = i_a(wt) \Big|_{wt = \alpha + 2\pi/3}$$

we get

$$i_a(wt) = \frac{E_m}{Z} \left[\sin(wt - \emptyset) - \frac{\sin(\alpha - \emptyset) e^{-\cot \emptyset (wt - \alpha - \pi/3)}}{1 - e^{-\cot \emptyset (\pi/3)}} \right] - \frac{E_d}{R_a} \quad (3.2)$$

Taking the base value of i_a as $\frac{3E_m}{\pi R_a}$, normalised Eqn.

(3.2) is given by

$$i_n(wt) = \frac{\pi}{3} \cos \emptyset \left[\sin(wt - \emptyset) - \frac{\sin(\alpha - \emptyset) e^{-\cot \emptyset (wt - \alpha - \pi/3)}}{1 - e^{-\cot \emptyset (\pi/3)}} \right] - WN \quad (3.3)$$

Mode 2: Fig. 3.3(b) Discontinuous Conduction with $\alpha < \gamma$

The system operation is described by the following equations:

$$L_a \frac{di_a}{dt} + i_a R_a + E_d = E_m \sin wt \quad \gamma + \pi/3 \leq wt \leq \alpha + 2\pi/3 \quad (3.4)$$

$$L_a \frac{di_a}{dt} + i_a R_a + E_d = E_m \sin(wt - \pi/3) \quad \alpha + 2\pi/3 \leq wt \leq \beta + \pi/3 \quad (3.5)$$

Solving (3.4) and (3.5) with the condition that

$$i_a(wt) \Big|_{wt = \gamma + \pi/3} = 0$$

we get the normalised solution as

$$i_n(wt) = \frac{\pi}{3} \cos \emptyset \left[\sin(wt - \emptyset) - \sin(\gamma + \pi/3 - \emptyset) e^{-\cot \emptyset (wt - \gamma - \pi/3)} \right] - WN \left[1 - e^{-\cot \emptyset (wt - \gamma - \pi/3)} \right] \quad (\gamma + \pi/3) \leq wt \leq (\alpha + 2\pi/3)$$

(3.6)

$$\begin{aligned}
i_n(\omega t) = & \frac{\pi}{3} \cos \theta [\sin(\omega t - \pi/3 - \theta) - \sin(\alpha - \theta)] \\
& e^{-\cot \theta (\omega t - \alpha - 2\pi/3)} \\
& - \sin(\gamma + \pi/3 - \theta) e^{-\cot \theta (\omega t - \gamma - \pi/3)} \\
& - \omega N [1 - e^{-\cot \theta (\omega t - \gamma - \pi/3)}] \\
& (\alpha + 2\pi/3) \leq \omega t \leq (\beta + \pi/3) \quad (3.7)
\end{aligned}$$

Mode 3: Fig. 3.3(d) Discontinuous conduction with $\alpha > \gamma$

The system operation is described by

$$L_a \frac{di_a}{dt} + i_a R_a + E_d = E_m \sin \omega t \quad \alpha + \pi/3 \leq \omega t \leq \beta + \pi/3 \quad (3.8)$$

Solving (3.8) with the condition that

$$i_a(\omega t) \big|_{\omega t = \alpha + \pi/3} = 0$$

we get the normalised solution as

$$\begin{aligned}
i_n(\omega t) = & \frac{\pi}{3} \cos \theta [\sin(\omega t - \theta) \\
& - \sin(\alpha + \pi/3 - \theta) e^{-\cot \theta (\omega t - \alpha - \pi/3)}] \\
& - \omega N [1 - e^{-\cot \theta (\omega t - \alpha - \pi/3)}] \\
& \alpha + \pi/3 \leq \omega t \leq \beta + \pi/3 \quad (3.9)
\end{aligned}$$

3.2(b) Half Controlled Operation

Mode 1: Continuous Conduction

(a) $\alpha < \pi/3$ (Figs. 3.2(a) and (b))

The system operation is described by

$$L_a \frac{di_a}{dt} + i_a R_a + E_d = E_m \sin wt$$

$$(\alpha + \pi/3) \leq wt \leq 2\pi/3 \quad (3.10)$$

$$L_a \frac{di_a}{dt} + i_a R_a + E_d = E_m \sin (wt - \pi/3)$$

$$2\pi/3 \leq wt \leq (\alpha + \pi) \quad (3.11)$$

Solving (3.10) and (3.11) with the condition that

$$i_a(wt) \big|_{wt = \alpha + \pi/3} = i_a(wt) \big|_{wt = \alpha + \pi}$$

we get the normalised current solution as:

$$i_n(wt) = \frac{\pi}{3} \cos \emptyset [\sin(wt - \emptyset) + \frac{\sin \emptyset e^{-\cot \emptyset (wt)} - \sin(\alpha - \emptyset) e^{-\cot \emptyset (wt - \alpha - \pi/3)}}{1 - e^{-\cot \emptyset (2\pi/3)}}] - WN$$

$$(\alpha + \pi/3) \leq wt \leq 2\pi/3 \quad (3.12)$$

$$i_n(wt) = \frac{\pi}{3} \cos \emptyset [\sin(wt - \pi/3 - \emptyset) + \frac{\sin \emptyset e^{-\cot \emptyset (wt - 2\pi/3)} - \sin(\alpha - \emptyset) e^{-\cot \emptyset (wt - \alpha - \pi/3)}}{1 - e^{-\cot \emptyset (2\pi/3)}}] - WN$$

$$2\pi/3 \leq wt \leq (\alpha + \pi) \quad (3.13)$$

(b) $\alpha > \pi/3$ (Fig. 3.2(c))

The system operation is described by the following equations:

$$L_a \frac{di_a}{dt} + i_a R_a + E_d = E_m \sin (wt - \pi/3)$$

$$\alpha + \pi/3 \leq wt \leq 4\pi/3 \quad (3.14)$$

$$L_a \frac{di_a}{dt} + i_a R_a + E_d = 0$$

$$4\pi/3 \leq wt \leq \alpha + \pi \quad (3.15)$$

Solving these equations with the condition that

$$i_a(wt) \Big|_{wt = \alpha + \pi/3} = i_a(wt) \Big|_{wt = \alpha + \pi}$$

we get the normalised solution as given by (3.13) for

$$(\alpha + \pi/3) \leq wt \leq 4\pi/3 \quad \text{and}$$

$$i_n(wt) = \frac{\pi}{3} \cos \emptyset \left[\sin \emptyset e^{-\cot \emptyset (wt - 4\pi/3)} \right.$$

$$\left. - \sin(\alpha - \emptyset) e^{-\cot \emptyset (wt - \alpha - \pi/3)} \right] /$$

$$(1 - e^{-\cot \emptyset (2\pi/3)}) - \omega N$$

$$4\pi/3 \leq wt \leq \alpha + \pi \quad (3.16)$$

Mode 2: Fig. 3.2(d) Discontinuous Conduction with $\alpha < \gamma$

The system operation is described by the equations:

$$L_a \frac{di_a}{dt} + i_a R_a + E_d = E_m \sin \omega t \quad (\gamma + \pi/3) \leq \omega t \leq 2\pi/3 \quad (3.17)$$

$$L_a \frac{di_a}{dt} + i_a R_a + E_d = E_m \sin(\omega t - \pi/3) \quad 2\pi/3 \leq \omega t \leq (\alpha + \pi) \quad (3.18)$$

$$L_a \frac{di_a}{dt} + i_a R_a + E_d = E_m \sin(\omega t - 2\pi/3) \quad (\alpha + \pi) \leq \omega t \leq (\beta + \pi/3) \quad (3.19)$$

initial condition

$$i_a(\omega t) \Big|_{\omega t = (\gamma + \pi/3)} = 0$$

$$\begin{aligned} i_n(\omega t) = & \frac{\pi}{3} \cos \emptyset [\sin(\omega t - \emptyset) \\ & - \sin(\gamma + \pi/3 - \emptyset) e^{-\cot \emptyset (\omega t - \gamma - \pi/3)}] \\ & - WN [1 - e^{-\cot \emptyset (\omega t - \gamma - \pi/3)}] \end{aligned} \quad (\gamma + \pi/3) \leq \omega t \leq 2\pi/3 \quad (3.20)$$

$$\begin{aligned} i_n(\omega t) = & \frac{\pi}{3} \cos \emptyset [\sin(\omega t - \pi/3 - \emptyset) \\ & + \sin \emptyset e^{-\cot \emptyset (\omega t - 2\pi/3)} \\ & - \sin(\gamma + \pi/3 - \emptyset) e^{-\cot \emptyset (\omega t - \gamma - \pi/3)}] \\ & - WN [1 - e^{-\cot \emptyset (\omega t - \gamma - \pi/3)}] \end{aligned} \quad 2\pi/3 \leq \omega t \leq (\alpha + \pi) \quad (3.21)$$

$$\begin{aligned}
i_n(wt) = & \frac{\pi}{3} \cos \emptyset [\sin(wt - 2\pi/3 - \emptyset) \\
& + \sin \emptyset e^{-\cot \emptyset (wt - 2\pi/3)} - \sin(\alpha - \emptyset) e^{-\cot \emptyset (wt - \alpha - \pi)} \\
& - \sin(\gamma + \pi/3 - \emptyset) e^{-\cot \emptyset (wt - \gamma - \pi/3)}] \\
& - WN [1 - e^{-\cot \emptyset (wt - \gamma + \pi/3)}] \\
& (\alpha + \pi) \leq wt \leq (\beta + \pi/3) \quad (3.22)
\end{aligned}$$

Mode 3: Fig. 3.2(f) Discontinuous Conduction with $\alpha < \pi/3$
and $\alpha > \gamma$

The system operation is discussed by:

$$L_a \frac{di_a}{dt} + i_a R_a + E_d = E_m \sin wt \quad \alpha + \pi/3 \leq wt \leq 2\pi/3 \quad (3.23)$$

$$\begin{aligned}
L_a \frac{di_a}{dt} + i_a R_a + E_d &= E_m \sin (wt - \pi/3) \\
2\pi/3 &\leq wt \leq (\beta + \pi/3) \quad (3.24)
\end{aligned}$$

initial condition:

$$i_a(wt) \Big|_{wt = \alpha + \pi/3} = 0$$

Solving (3.23) and (3.24) with the above condition we get

$$\begin{aligned}
i_n(wt) = & \frac{\pi}{3} \cos \emptyset [\sin(wt - \emptyset) \\
& - \sin(\alpha + \pi/3 - \emptyset) e^{-\cot \emptyset (wt - \alpha - \pi/3)}] \\
& - WN [1 - e^{-\cot \emptyset (wt - \alpha - \pi/3)}] \\
& \alpha + \pi/3 \leq wt \leq 2\pi/3 \quad (3.25)
\end{aligned}$$

$$\begin{aligned}
i_n(\omega t) = & \frac{\pi}{3} \cos \emptyset [\sin(\omega t - \pi/3 - \emptyset) \\
& + \sin \emptyset e^{-\cot \emptyset (\omega t - 2\pi/3)} \\
& - \sin(\alpha + \pi/3 - \emptyset) e^{-\cot \emptyset (\omega t - \alpha - \pi/3)}] \\
& - \omega N [1 - e^{-\cot \emptyset (\omega t - \alpha - \pi/3)}] \\
& 2\pi/3 \leq \omega t \leq (\beta + \pi/3) \quad (3.26)
\end{aligned}$$

Mode 4: Fig. 3.2(g) Discontinuous Conduction with $\alpha < \pi/3$

The system operation is described by:

$$\begin{aligned}
L_a \frac{di_a}{dt} + i_a R_a + E_d &= E_m \sin \omega t \\
(\alpha + \pi/3) \leq \omega t \leq (\beta_1 + \pi/3) \quad (3.27)
\end{aligned}$$

$$\begin{aligned}
L_a \frac{di_a}{dt} + i_a R_a + E_d &= E_m \sin (\omega t - \pi/3) \\
(\gamma + 2\pi/3) \leq \omega t \leq (\beta_2 + \pi/3) \quad (3.28)
\end{aligned}$$

initial conditions

$$i_a(\omega t) \Big|_{\omega t = \alpha + \pi/3} = 0$$

$$i_a(\omega t) \Big|_{\omega t = \gamma + 2\pi/3} = 0$$

Solving (3.27) and (3.28) with the above conditions the solution is given by (3.25) for $(\alpha + \pi/3) \leq \omega t \leq (\beta_1 + \pi/3)$

and

$$\begin{aligned}
 i_n(\omega t) &= \frac{\pi}{3} \cos \emptyset [\sin(\omega t - \pi/3 - \emptyset) \\
 &\quad - \sin(\gamma + \pi/3 - \emptyset) e^{-\cot \emptyset (\omega t - \gamma - 2\pi/3)}] \\
 &\quad - \omega N [1 - e^{-\cot \emptyset (\omega t - \gamma - 2\pi/3)}] \\
 &\quad (\gamma + 2\pi/3) \leq \omega t \leq (\beta_2 + \pi/3) \quad (3.29)
 \end{aligned}$$

Mode 5: Fig. 2(k) Discontinuous Conduction with

$$\alpha < \pi/3 \text{ and } \alpha > \gamma$$

The system operation is described by:

$$\begin{aligned}
 L_a \frac{di_a}{dt} + i_a R_a + E_d &= E_m \sin \omega t \\
 \alpha + \pi/3 &\leq \omega t \leq 2\pi/3 \quad (3.30)
 \end{aligned}$$

$$\begin{aligned}
 L_a \frac{di_a}{dt} + i_a R_a + E_d &= E_m \sin(\omega t - \pi/3) \\
 2\pi/3 &\leq \omega t \leq (\beta_1 + \pi/3) \quad (3.31)
 \end{aligned}$$

$$\begin{aligned}
 L_a \frac{di_a}{dt} + i_a R_a + E_d &= E_m \sin(\omega t - \pi/3) \\
 (\gamma + 2\pi/3) &\leq \omega t \leq (\beta_2 + \pi/3) \quad (3.32)
 \end{aligned}$$

initial conditions:

$$i_a(\omega t) \big|_{\omega t = \alpha + \pi/3} = 0$$

$$i_a(\omega t) \big|_{\omega t = \gamma + 2\pi/3} = 0$$

Solving (3.30), (3.31) and (3.32) with the help of the above conditions the normalised solutions are given by

$$(3.25) \text{ for } (\alpha + \pi/3) \leq \omega t \leq 2\pi/3$$

$$(3.26) \text{ for } (2\pi/3) \leq \omega t \leq (\beta_1 + \pi/3)$$

$$\text{and } (3.29) \text{ for } (\gamma + 2\pi/3) \leq \omega t \leq (\beta_2 + \pi/3)$$

Mode 6: Fig. 3.2(i) Discontinuous Conduction with

$$(\pi/3 - \gamma) \leq \omega t \leq (\gamma + \pi/3)$$

The system operation is described by

$$L_a \frac{di_a}{dt} + i_a R_a + E_d = E_m \sin (\omega t - \pi/3)$$

$$(\gamma + 2\pi/3) \leq \omega t \leq (\beta + \pi/3) \quad (3.33)$$

initial condition:

$$i_a(\omega t) \Big|_{\omega t = \gamma + 2\pi/3} = 0$$

Solving (3.33) with the above condition the solution is given by (3.29) for $(\gamma + 2\pi/3) \leq \omega t \leq (\beta + \pi/3)$

Mode 7: Fig. 3.2(j) Discontinuous with $\alpha > \pi/3$ and $\beta < \pi$

The system operation is described by

$$L_a \frac{di_a}{dt} + i_a R_a + E_d = E_m \sin (\omega t - \pi/3)$$

$$(\alpha + \pi/3) \leq \omega t \leq (\beta + \pi/3) \quad (3.34)$$

initial condition:

$$i_a(\omega t) \Big|_{\omega t = \alpha + \pi/3} = 0$$

Solving (3.34) with the above condition we get:

$$\begin{aligned}
 i_n(wt) = & \frac{\pi}{3} \cos \emptyset [\sin (wt - \pi/3 - \emptyset) \\
 & - \sin (\alpha - \emptyset) e^{-\cot \emptyset (wt - \alpha - \pi/3)}] \\
 & - WN [1 - e^{-\cot \emptyset (wt - \alpha - \pi/3)}] \\
 & (\alpha + \pi/3) \leq wt \leq (\beta + \pi/3) \quad (3.35)
 \end{aligned}$$

Mode 8: Fig. 3.2(k) Discontinuous Conduction with

$$\alpha > \pi/3 \text{ and } \beta < \pi$$

The system operation is described by

$$\begin{aligned}
 L_a \frac{di_a}{dt} + i_a R_a + E_d = E_m \sin(wt - \pi/3) \\
 (\alpha + \pi/3) \leq wt \leq (4\pi/3) \quad (3.36)
 \end{aligned}$$

$$L_a \frac{di_a}{dt} = i_a R_a + E_d = 0 \quad 4\pi/3 \leq wt \leq (\beta + \pi/3) \quad (3.37)$$

initial condition:

$$i_a(wt) \Big|_{wt = \alpha + \pi/3} = 0$$

Solving (3.36) and (3.37) with the above condition the solution is given by (3.35) for $(\alpha + \pi/3) \leq wt \leq 4\pi/3$ and

$$\begin{aligned}
 i_n(wt) = & \frac{\pi}{3} \cos \emptyset [\sin \emptyset e^{-\cot \emptyset (wt - 4\pi/3)} \\
 & - \sin(\alpha - \emptyset) e^{-\cot \emptyset (wt - \alpha - \pi/3)}] \\
 & - WN [1 - e^{-\cot \emptyset (wt - \alpha - \pi/3)}] \\
 & 4\pi/3 \leq wt \leq (\beta + \pi/3) \quad (3.38)
 \end{aligned}$$

3.3 BOUNDARY BETWEEN CONTINUOUS AND DISCONTINUOUS CONDUCTION

For a particular phase angle and given firing angle the critical speed WNC, representing the boundary between continuous and discontinuous condition, is obtained by letting the conduction period to be $\pi/3$ for fully controlled operation and $2\pi/3$ for half controlled operation. The expressions representing critical conditions are as given below. The critical torque, below which discontinuous conduction takes place is also given.

3.3 (a) Fully Controlled Operation

Mode 2:

The critical speed for $\alpha < \gamma$ is obtained by letting

$$i_a(\omega t) \Big|_{\omega t = \gamma + 2\pi/3} = 0 \text{ in (3.7).}$$

Thus

$$\begin{aligned} \text{WNC} = \frac{\pi}{3} \cos \emptyset \Big[& \sin (\gamma + \pi/3 - \emptyset) \\ & - \frac{\sin(\alpha - \emptyset) e^{-\cot \emptyset (\gamma - \beta)}}{1 - e^{-\cot \emptyset (\pi/3)}} \Big] \end{aligned} \quad (3.39(a))$$

also

$$\text{WNC} = \frac{\pi}{3} \sin (\gamma + \pi/3) \quad (3.39(b))$$

$$\text{TNC} = \cos \alpha - \text{WNC} \quad (3.40)$$

Mode 3:

The critical speed for $\alpha > \gamma$ is obtained by letting

$$i_a(\omega t) \big|_{\omega t = \alpha + 2\pi/3} = 0 \text{ in (3.9)}$$

$$\begin{aligned} \text{WNC} = \frac{\pi}{3} \cos \phi [\sin(\alpha + \pi/3 - \phi) \\ - \sin(\alpha + \pi/3 - \phi) e^{-\cot \phi (\pi/3)}] / [1 - e^{-\cot \phi (\pi/3)}] \end{aligned} \quad (3.41)$$

The critical torque is given by (3.40)

3.3 (b) Half Controlled Operation

Mode 2: The critical speed for $\alpha < \gamma$ is calculated by letting

$$i_a(\omega t) \big|_{\omega t = (\gamma + \pi)} = 0 \text{ in (3.22) giving}$$

$$\begin{aligned} \text{WNC} = \frac{\pi}{3} \cos \phi [\sin(\gamma + \pi/3 - \phi) \\ + \frac{\sin \phi e^{-\cot \phi (\gamma + \pi/3)} - \sin(\alpha - \phi) e^{-\cot \phi (\gamma - \alpha)}}{1 - e^{-\cot \phi (2\pi/3)}}] \end{aligned} \quad (3.42(a))$$

$$\text{WNC} = \frac{\pi}{3} \sin(\gamma + \pi/3) \quad (3.42(b))$$

$$\text{TNC} = \frac{1 + \cos \alpha}{2} - \text{WNC} \quad (3.43)$$

Mode 3: The critical speed for $\alpha > \gamma$ and $\alpha < \pi/3$ is obtained by letting

$$i_a(\omega t) \big|_{\omega t = \alpha + \pi} = 0 \text{ in (3.26),}$$

thus,

$$\begin{aligned} WNC = \frac{\pi}{3} \cos \emptyset \left[\sin(\alpha + 2\pi/3 - \emptyset) + \right. \\ \left. \sin \emptyset e^{-\cot \emptyset (\alpha + \pi/3)} \right. \\ \left. - \sin(\alpha + \pi/3 - \emptyset) e^{-\cot \emptyset (2\pi/3)} \right] / [1 - e^{-\cot \emptyset (2\pi/3)}] \end{aligned} \quad (3.44)$$

The critical torque is given by (3.43)

Mode 8: The critical torque for $\alpha > \pi/3$ is calculated by letting

$$i_a(wt) \Big|_{wt = \alpha + \gamma} = 0 \text{ in (3.38)}$$

which gives

$$\begin{aligned} WNC = \frac{\pi}{3} \cos \emptyset \left[\sin \emptyset e^{-\cot \emptyset (\alpha - \pi/3)} \right. \\ \left. - \sin(\alpha - \emptyset) e^{-\cot \emptyset (2\pi/3)} \right] / [1 - e^{-\cot \emptyset (2\pi/3)}] \end{aligned} \quad (3.45)$$

The critical torque is given by (3.43).

Using these expressions, a set of boundaries for various values of \emptyset are computed as shown in Fig. 3.4. Area is the left of the boundary gives discontinuous conduction. These boundaries are used for choosing the value of filter inductance with a view to eliminate discontinuous conduction, as described later.

3.4 METHOD OF MODE SELECTION

3.4 (a) Fully Controlled Operation

The method of mode selection is given in the flow chart of Fig. 3.5(a). For a particular value of \emptyset and α , we first find the critical speed as described in Section 3.3. For the given value of speed W_N , we find whether it is greater or less than the critical speed. If W_N is equal to W_{NC} it signifies critical condition. If W_N is less than W_{NC} , it signifies continuous conduction. For both these conditions Eqn. (3.3) will give us the instantaneous values of armature current for $wt = \alpha + \pi/3$ to $wt = \alpha + 2\pi/3$. Similarly we get the instantaneous value of the armature output voltage. The average of the product of these two gives us the average power output.

To find the source current for half a cycle we have the following conditions:

$$\begin{aligned} i_{sn}(wt) &= i_n(wt) && \text{for } \alpha + \pi/3 \leq wt \leq \alpha + 2\pi/3 \\ i_{sn}(wt) &= i_{sn}(wt - \pi/3) && \text{for } \alpha + 2\pi/3 \leq wt \leq \alpha + \pi \\ i_{sn}(wt) &= 0 && \text{for } \alpha + \pi \leq wt \leq \alpha + 4\pi/3 \end{aligned} \quad (3.46)$$

If, however, W_N is greater than W_{NC} , it signifies discontinuous conduction condition. At this stage we need to find if α is less than γ or not. If $\alpha < \gamma$ it signifies operation under Mode 2 and Eqns. (3.6) and (3.7) give us the current values for $(\gamma + \pi/3) \leq wt \leq (\beta + \pi/3)$.

From $(\beta + \pi/3)$ to $(\gamma + 2\pi/3)$ we have $i_n(wt) = 0$.

The instantaneous values of converter output voltage is also obtained for the duration and the average power output is calculated. The source current solution is also obtained as given in (3.46) with $\alpha = \gamma$.

If under discontinuous conduction, α is greater than γ , the same operations are carried out as given above. The operation now is under mode 3 and using Eqn. (3.9) we get $i_n(wt)$ for $\alpha + \pi/3 \leq wt \leq \beta + \pi/3$ and $i_n(wt) = 0$ for $\beta + \pi/3 \leq wt \leq \alpha + 2\pi/3$. The average output power is calculated similarly and the source current is obtained using Eqn. (3.46).

3.4 (b) Half Controlled Operation

The mode is selected under half controlled operation using the flow chart given in Fig. 3.5(b). For a particular value of \emptyset and α , the critical speed is found as described in Section 3.3. For the given value of speed WN , γ is calculated. If

$$(\pi/3 - \gamma) < \alpha < (\pi/3 + \gamma) \quad (3.47)$$

WN is compared with WNC . If $WN > WNC$ it means discontinuous conduction operation under Mode 6 and Eqn. (3.29) gives the instantaneous value of $i_n(wt)$ for $(\gamma + 2\pi/3) \leq wt \leq (\beta + \pi/3)$ and $i_n(wt) = 0$ for $(\beta + \pi/3) \leq wt \leq (\gamma + 4\pi/3)$. The converter output voltage is obtained and the average

power output is calculated. The source current is given by:

$$\begin{aligned} i_{sn}(wt) &= i_n(wt) & (\alpha + 2\pi/3) \leq wt \leq (\alpha + 4\pi/3) \\ i_{sn}(wt) &= 0 & (\alpha + 4\pi/3) \leq wt \leq (\alpha + 5\pi/3) \end{aligned} \quad (3.48)$$

with $\alpha = \gamma$ in this case.

If $WN \leq WNC$, α is checked to see if it is less than or greater than $\pi/3$. If $\alpha < \pi/3$, it implies continuous conduction and Eqns. (3.12) and (3.13) give the armature current for $wt = (\alpha + \pi/3)$ to $wt = (\alpha + \pi)$. If $\alpha > \pi/3$ Eqns. (3.13) and (3.16) provide the solution. The source current is found using (3.48).

If, however, α is not within the range given by (3.47) and if $WN > WNC$ it is checked to see if $\alpha > \pi/3$ or not. If $\alpha < \pi/3$, α is again checked to see if $\alpha > \gamma$ or not. If $\alpha < \gamma$ it means discontinuous conduction under mode 2, and Eqns. (3.21) and (3.22) then give the solution for $i_n(wt)$ for $(\gamma + \pi/3) \leq wt \leq (\beta + \pi/3)$ and $i_n(wt) = 0$ for $(\beta + \pi/3) \leq wt \leq (\gamma + \pi)$. The instantaneous converter output voltage is calculated and the average power output is also calculated. Eqn. (3.48) gives the source current with $\alpha = \gamma$.

If $\alpha > \gamma$ and $\alpha < \pi/3$, $i_n(wt)$ is found using Eqn. (3.25) at $wt = 2\pi/3$. If $i_n(wt) < 0$ it means there is no current at $wt = 2\pi/3$ and discontinuous conduction takes place under Mode 4. Then, Eqns. (3.25) and (3.29) give the solution with $i_n(wt) = 0$ for $(\beta_1 + \pi/3) \leq wt \leq (\gamma + 2\pi/3)$ and for $(\beta_2 + \pi/3) \leq wt \leq (\alpha + \pi)$. Eqn. (3.48) gives the source current.

If $i_n(wt)$ at $wt = 2\pi/3$ using Eqn. (3.25) is greater than zero, $i_n(wt)$ is checked at $wt = \gamma + 2\pi/3$ using Eqn. (3.26). If $i_n(wt) < 0$ it implies discontinuous conduction under Mode 5 and Eqns. (3.25), (3.26) and (3.29) provide the solution within the prescribed limits and $i_n(wt) = 0$ for $(\beta_1 + \pi/3) \leq wt \leq (\gamma + 2\pi/3)$ and for $(\beta_2 + \pi/3) \leq wt \leq (\alpha + \pi)$. Eqn. (3.48) gives the source current.

However, if $i_n(wt) > 0$ at $wt = \gamma + 2\pi/3$, in Eqn. (3.26) it implies discontinuous conduction under Mode 3 and Eqns. (3.25) and (3.26) give the solution for $(\alpha + \pi/3) \leq wt \leq (\beta + \pi/3)$ and $i_n(wt) = 0$ for $(\beta + \pi/3) \leq wt \leq (\alpha + \pi)$. The source current is found using Eqn. 3.48. The instantaneous values of converter output voltage is also calculated.

The above discontinuous conduction modes are with $\alpha < \pi/3$. If $\alpha > \pi/3$ and $WN > WNC$, $i_n(wt)$ is found at $wt = 4\pi/3$ using Eqn. (3.35). If $i_n(wt) > 0$ it means operation under Mode 8 where Eqns. (3.35) and (3.38) give the

solution for armature current. If $i_n(wt) < 0$ it means operation under Mode 7 and Eqn. (3.35) gives the solution. Eqn. (3.48) gives the source current. The converter output voltage for this range is found.

3.5 PERFORMANCE COMPUTATIONS

3.5 (a) Speed-Torque Characteristics

For particular values of \emptyset and α , depending upon the speed WN , the system operates under a certain mode. The mode is selected in accordance with the method described in Section 3.4. The instantaneous values of armature current is determined.

The average of the armature current is found out numerically. Under normalised conditions, the torque is equal to the average armature current. Thus for a given speed WN , we can get the torque TN .

The flow-chart given in Fig. 3.6 is used to determine the speed torque characteristics for different phase angle values over the whole operating range.

Fig. 3.7 shows the speed-torque curves for different values of \emptyset . These curves can be directly used to determine the speed torque characteristics for any motor, as they are plotted on normalised axes.

CENTRAL LIBRARY

Ac- No. 82647

3.5(b) Load Current Ripple

The load current ripple is defined by the following equation:

$$\text{Ripple factor} = \text{RF} = \frac{i_{\max} - i_{\min}}{2} \quad (3.49)$$

So long as the load current is continuous, the current ripple is independent of the variation in the motor back emf. The change in the back emf affects only the d.c. component of load current.

For particular values of δ and α , the instantaneous current values are computed, (as described in Section 3.4) for a value of speed, chosen to ensure continuous conduction. The maximum and minimum current values are noted and the ripple factor found. This operation is carried over the full operating range for a particular value of δ . The maximum ripple factor is thus determined.

Fig. 3.8 shows a flow chart for computations of maximum ripple factor for different values of δ . Fig. 3.9 shows the variation of the maximum ripple factor with different values of δ . This can be directly used to determine the maximum ripple factor for any motor.

3.5(c) Power-Factor

The power factor for converter fed drives is defined by the following equation:

$$\begin{aligned}
 \text{Power-factor} = \text{PF} &= \frac{\text{Input power}}{\text{Volt ampere input}} \\
 &= \frac{\text{input power}}{\text{rms input voltage} \times \text{rms source current}}
 \end{aligned}
 \tag{3.50}$$

As the devices are assumed to be ideal, the input power is equal to the output power of the converter.

For particular values of \emptyset and α , depending upon the value of speed WN , the mode of operation is determined as described in Section 3.4. The instantaneous values of armature current, source current and the converter output voltage are determined. The average of the product of the armature current and converter voltage output is computed using numerical techniques. This gives the average power output of the converter which is equal to the input power to the converter. The rms value of the source current is also computed. The line to line normalised rms voltage is given by $\pi/3\sqrt{2}$ and the apparent power is given by the following equation:

$$\text{Apparent power} = \sqrt{3} \times \frac{\pi}{3\sqrt{2}} \times i_{\text{rms}} = \frac{\pi}{\sqrt{6}} \times i_{\text{rms}} \tag{3.51}$$

Thus having computed the input real and apparent power the power factor can be calculated using Eqn. (3.50).

The flow-chart shown in Fig. 3.6, is used for the computations of power factor. Fig. 3.10 shows the power-factor variation with $\phi = 1.4$. The same approach can be easily extended for any desired phase angle value.

3.5(d) Distortion-Factor and Harmonic Contents in Source Current

The line current distortion factor is defined by

$$\text{distortion factor} = \text{DF} = \frac{\text{rms value of fundamnent component}}{\text{rms value of line current}} \quad (3.52)$$

The rms value of the n^{th} harmonic is given by:

$$n^{\text{th}} \text{ harmonic rms} = \sqrt{\frac{a_n^2 + b_n^2}{2}} \quad (3.53)$$

where

$$a_n = \frac{\pi}{2} \int_0^{\pi} i_n(\omega t) \cos n\omega t \, d\omega t \quad (3.54)$$

$$b_n = \frac{\pi}{2} \int_0^{\pi} i_n(\omega t) \sin n\omega t \, d\omega t \quad (3.55)$$

For particular values of ϕ and α the mode is identified for a given WN . The instantaneous source current values are computed (as described in Section 3.4). Using Eqs. (3.53), (3.54) and (3.55) the fundamental component and the different harmonics are calculated using numerical integration. The rms value of the source current is also computed. Using Eqn. (3.52) the distortion factor is calculated. Flow chart for calculation of distortion factor is given in Fig. 3.6.

Fig. 3.11 shows the distortion factor variation with load current for $\phi = 1.4$. Fig. 3.12 shows the different harmonic contents in the source current. The same approach can be easily extended for any desired phase angle value. The harmonic spectra for three-phase half controlled converter, under constant load conditions is given by Moltgen [9].

3.6 CHOICE OF FILTER INDUCTANCE

The filter inductance is chosen such that the motor current is continuous at all speeds and loads at which it may operate. Since discontinuous conduction occurs at light loads, if continuous conduction is assured for minimum loads at various speeds, the load current will be continuous at all loads and speeds at which the motor may operate. Therefore, from load requirement for a particular application under consideration minimum values of developed torque are obtained for various speeds and are superposed on the curves of Figs. 3.4(a) and 3.4(b). This is shown by chain dotted line. The filter inductor is chosen such that the boundary between continuous and discontinuous conduction falls to the left of this curve. In case the motor is likely to operate under no load, viscous and coulomb friction will provide the minimum load. Once the continuity of motor current is ensured the current ripple is calculated.

Since we know the motor armature resistance and inductance, we can calculate the extra inductance needed to avoid discontinuous conduction. If, however, the current ripple is not within permissible limits, a higher value of inductance is chosen.

Example

It is required to choose a filter inductance for a 3 HP, separately excited d.c. motor, whose specifications are given in Appendix. It is desired that the discontinuity in current be completely eliminated and the maximum current ripple be within 5 percent. The minimum load on the motor is assured to be 20 percent of the full load torque.

The chain dotted curve in Figs. 3.4(a) and (b) is the speed versus minimum load on the motor which includes a 20 percent of full load torque on the motor shaft and the coulomb and viscous friction losses. Since the discontinuity of armature current has to be completely eliminated, the filter inductance has to be chosen such that the boundary between continuous and discontinuous currents lies to be left of the chain dotted curve. Thus for fully controlled converter driven motor, from Fig. 3.4(a) the armature circuit specification is given by:

$$\phi = 1.24$$

$$\text{i.e. } \frac{L_a}{R_a} = 9.27 \text{ ms}$$

From Fig. 3.9(a) the corresponding maximum current ripple is given by,

$$CR = 2.3 \%$$

which is well within the permissible limit. Thus external inductance to be added = 1 mH

For half controlled converter driven motor, from Fig. 3.4(b)

$$\phi = 1.42$$

$$\text{i.e.} \quad \frac{L_a}{R_a} = 21 \text{ ms}$$

From Fig. 3.9(b), the corresponding maximum current is given by

$$CR = 2.3 \%$$

which is well within the permissible limit. Thus the external inductance to be inserted = 24.5 mH

The inductance required for half controlled converter to achieve same performance objective relating to continuous conduction and current ripple is more compared to that needed by fully controlled converter.

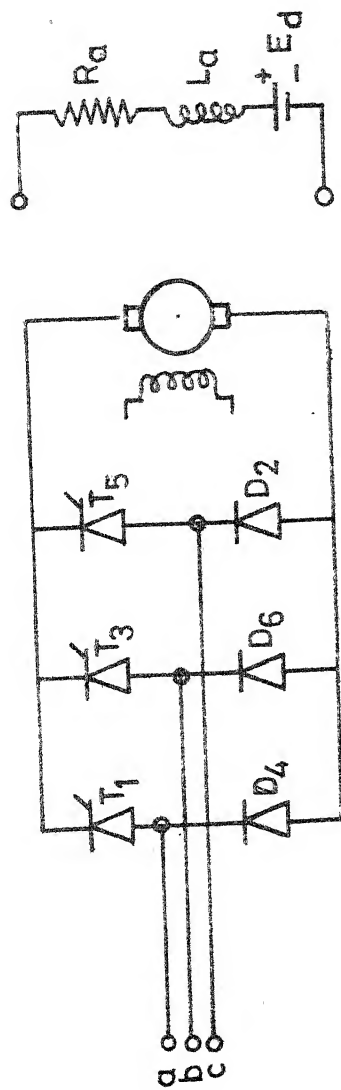


FIG.3.1(a) 3-PHASE HALF CONTROLLED CONVERTER FED D.C SEPERATELY EXCITED MOTOR

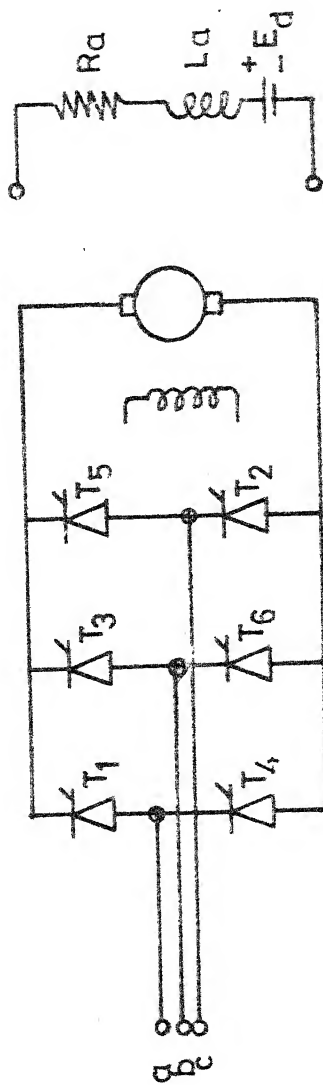


FIG.3.1(b) 3-PHASE FULLY CONTROLLED CONVERTER FED D.C SEPERATELY EXCITED MOTOR

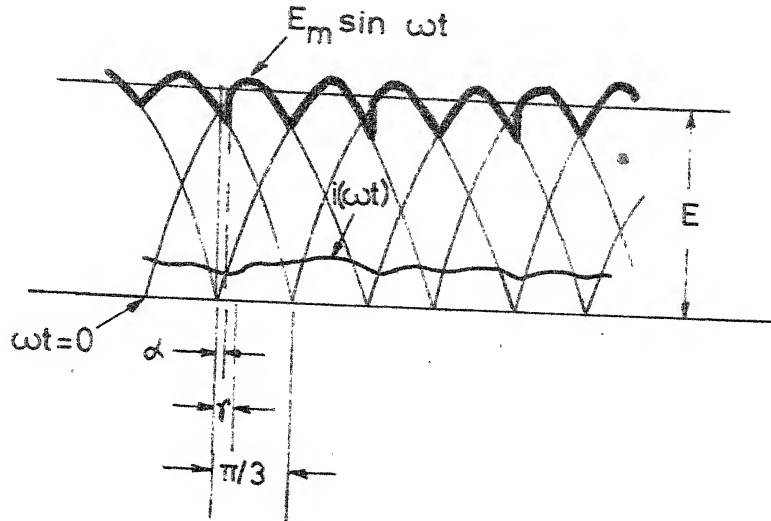


Fig. 3.2 (a) MODE 1 $\alpha < \gamma$

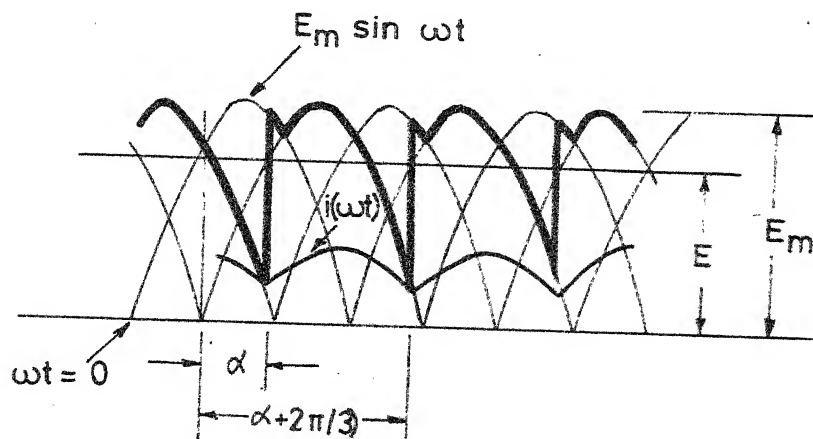


Fig. 3.2 (b) MODE 1

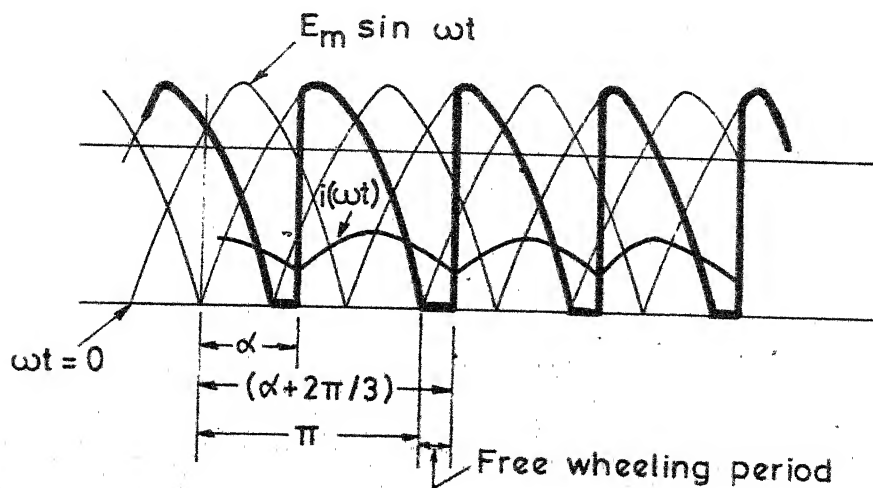


Fig. 3.2(c) MODE 1

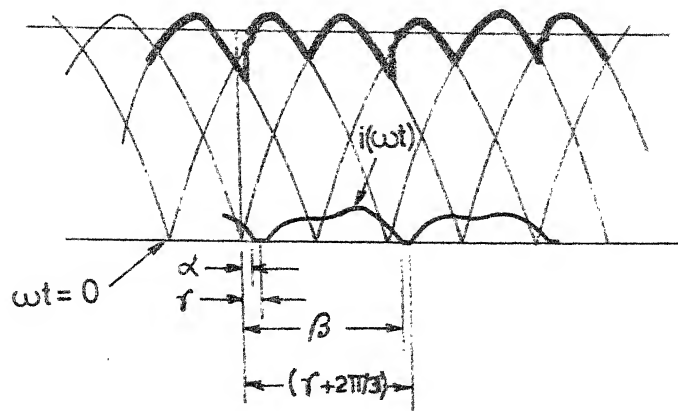


Fig. 3.2(d) MODE 2

$$\alpha < \tau$$

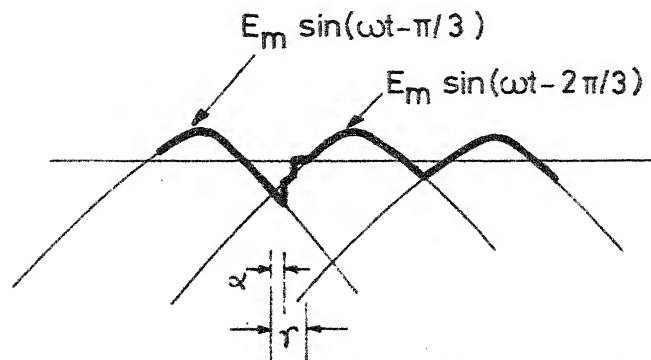


Fig. 3.2(e) ENLARGED VIEW

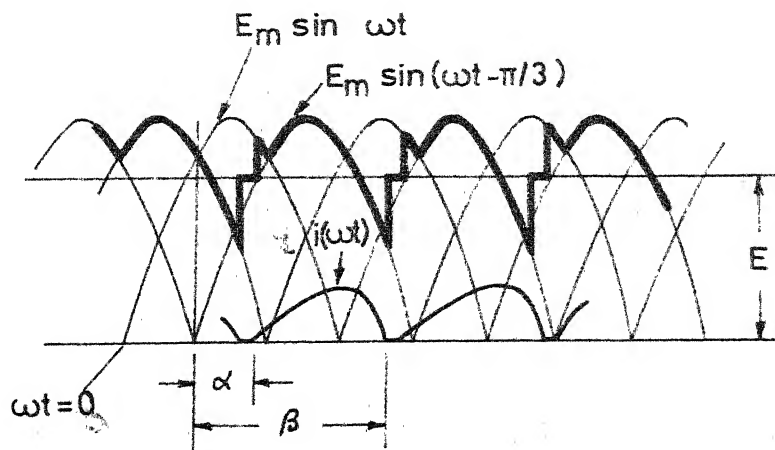


Fig. 3.2(f) MODE 3

$$\gamma < \alpha < \pi/3$$

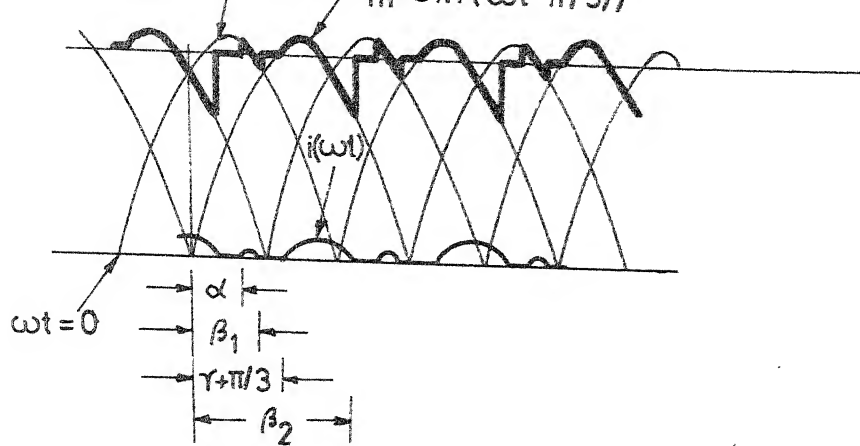


Fig.3.2(g) MODE 4 $\gamma < \alpha < \pi/3$

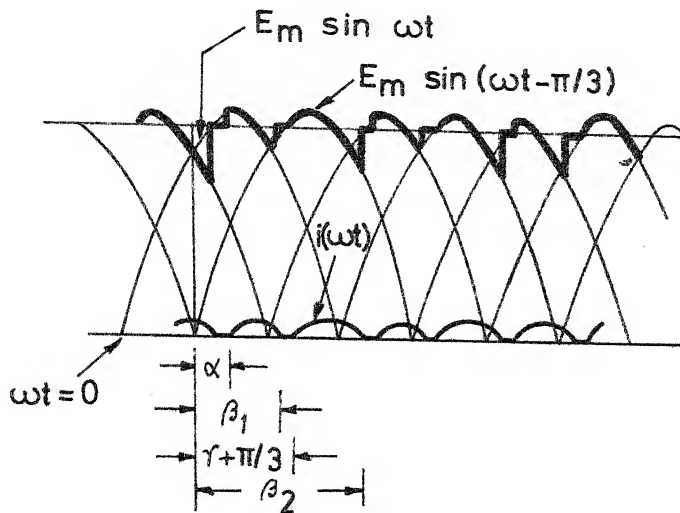


Fig. 3 2 (h) MODE 5 $\gamma < \alpha < \pi/3$

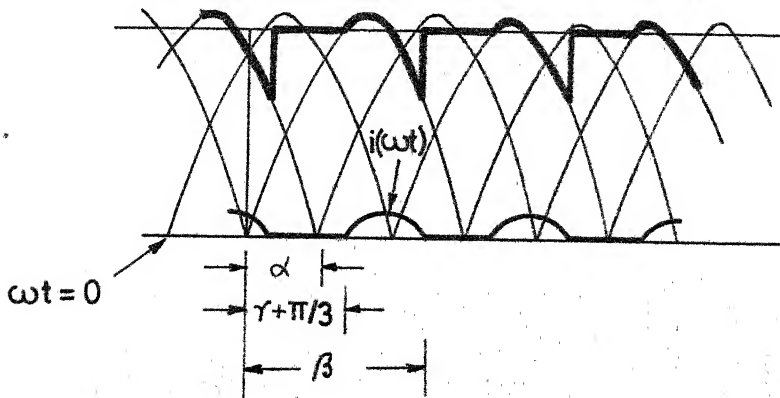


Fig. 3.2(i) MODE 6 $(\pi/3 - \gamma) \leq \alpha \leq (\pi/3 + \gamma)$

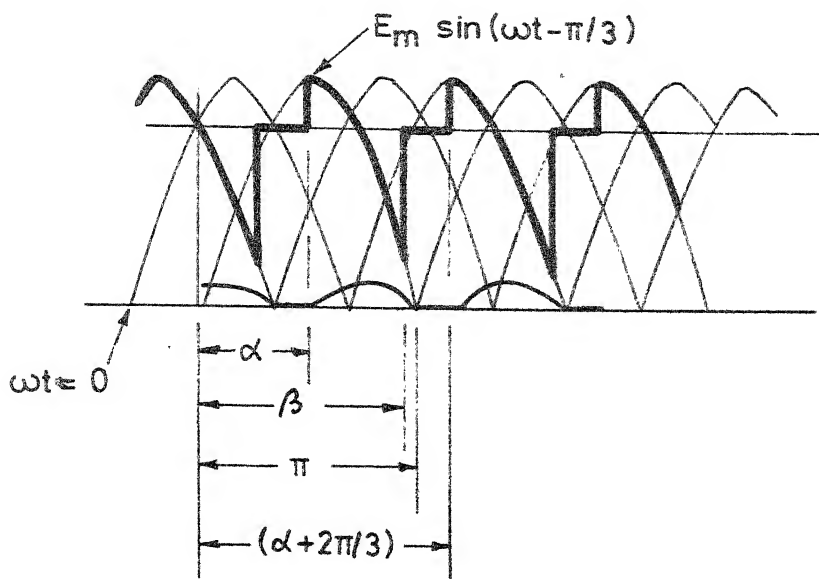


Fig . 3.2 (j) MODE 7

$$\alpha > \pi/3$$

$$\beta < \pi$$

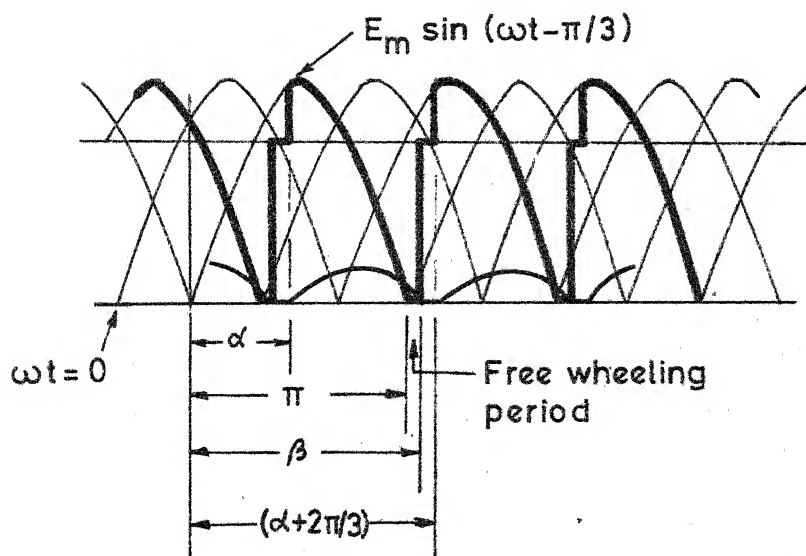


Fig.3.2(k) MODE 8

$$\alpha > \pi/3$$

$$\beta > \pi$$

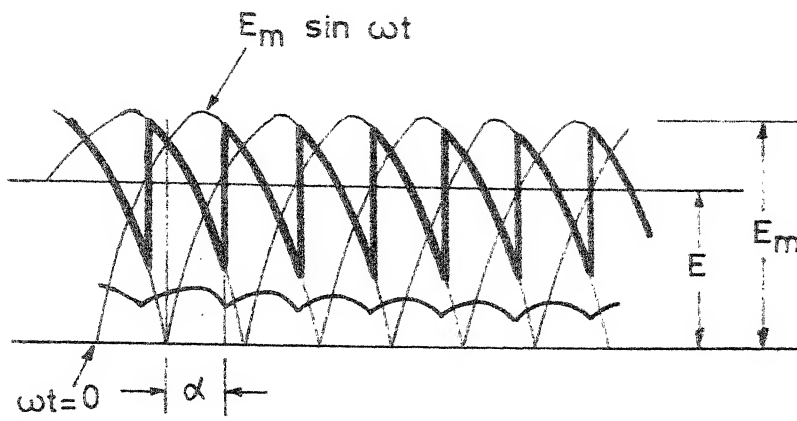


Fig. 3.3(a) MODE 1

$$\alpha > \gamma$$

or

$$\alpha < \gamma$$

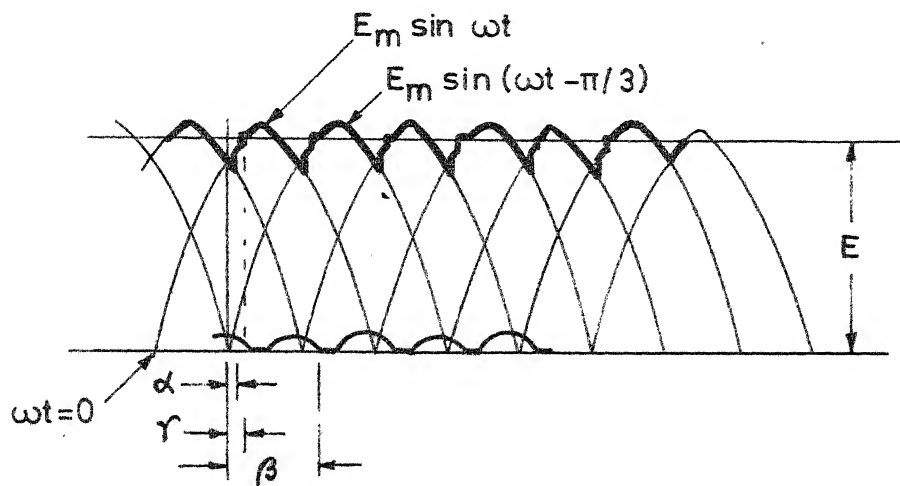


Fig. 3.3(b) MODE 2

$$\alpha < \gamma$$

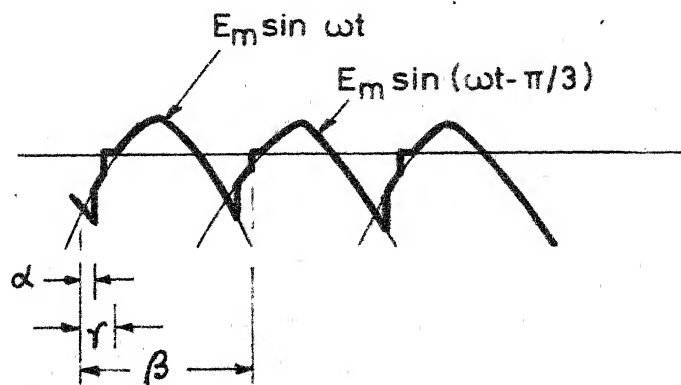


Fig. 3.3(c) ENLARGED VIEW

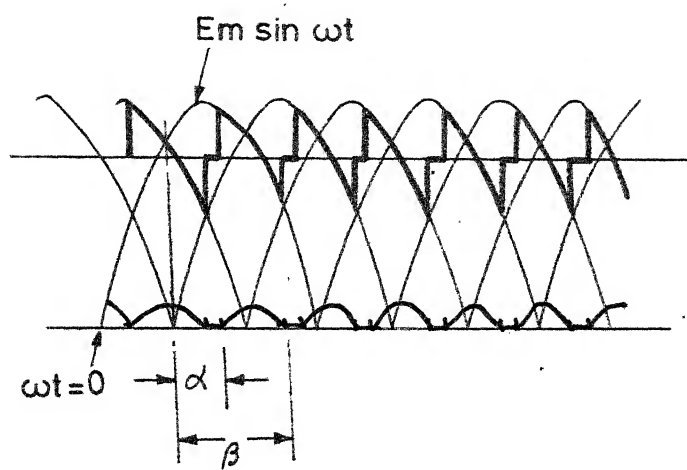


Fig. 3.3 (d) MODE 3 $\alpha > \gamma$

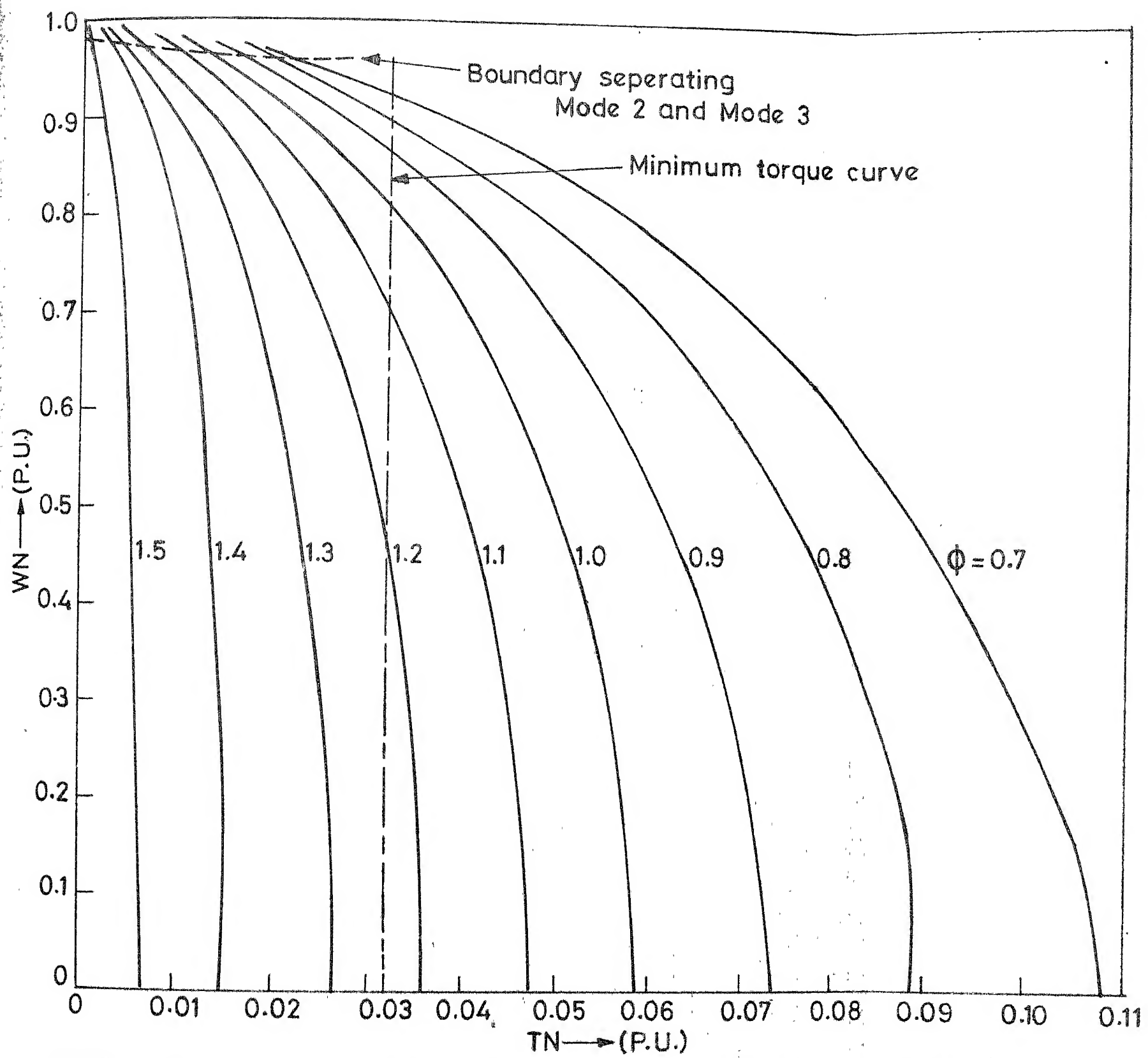


FIG. 3.4 (c) BOUNDARIES BETWEEN CONTINUOUS AND DISCONTINUOUS

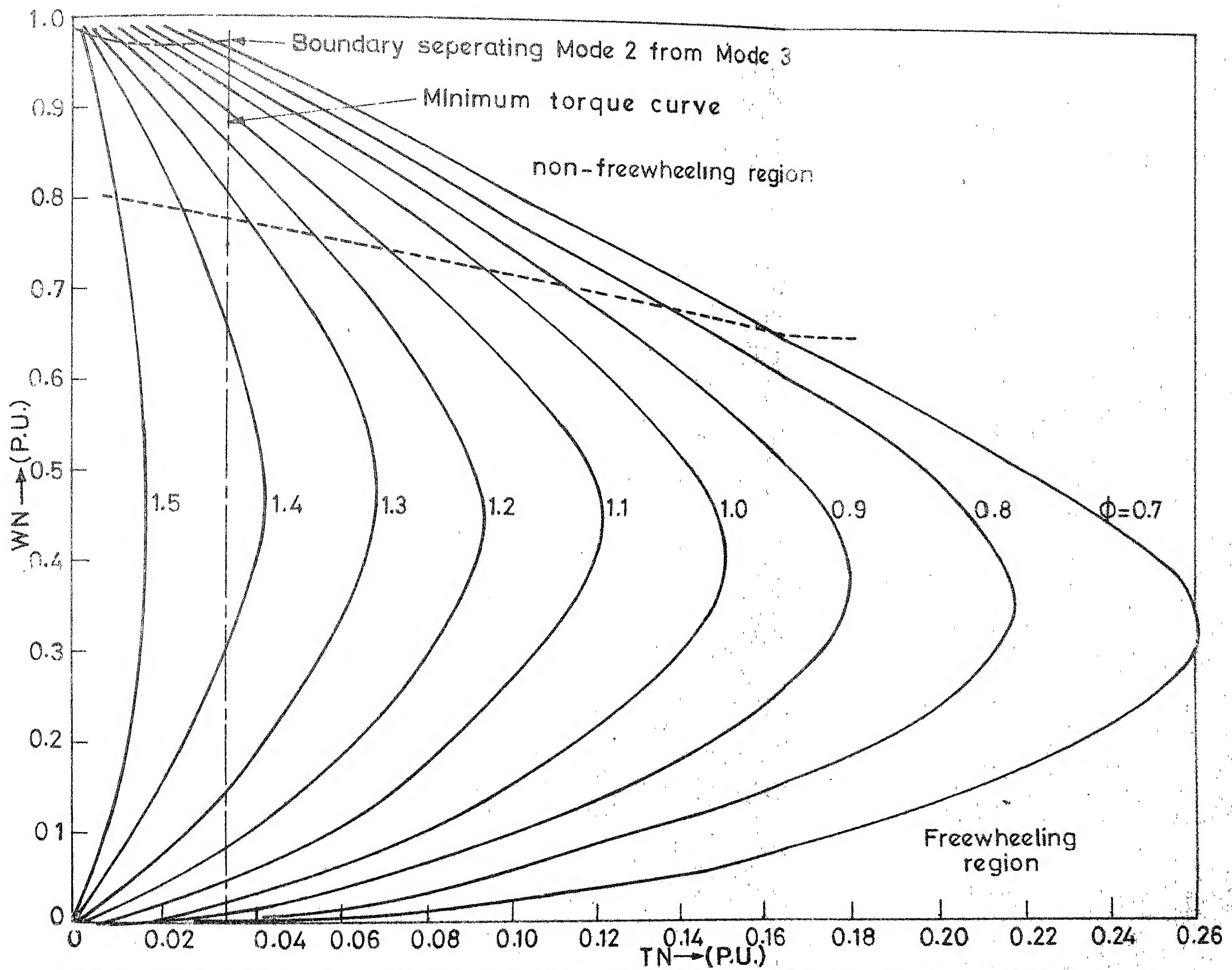


FIG.3.4(b) BOUNDARIES BETWEEN DISCONTINUOUS AND CONTINUOUS CONDUCTION FOR HALF CONTROLLED OPERATION

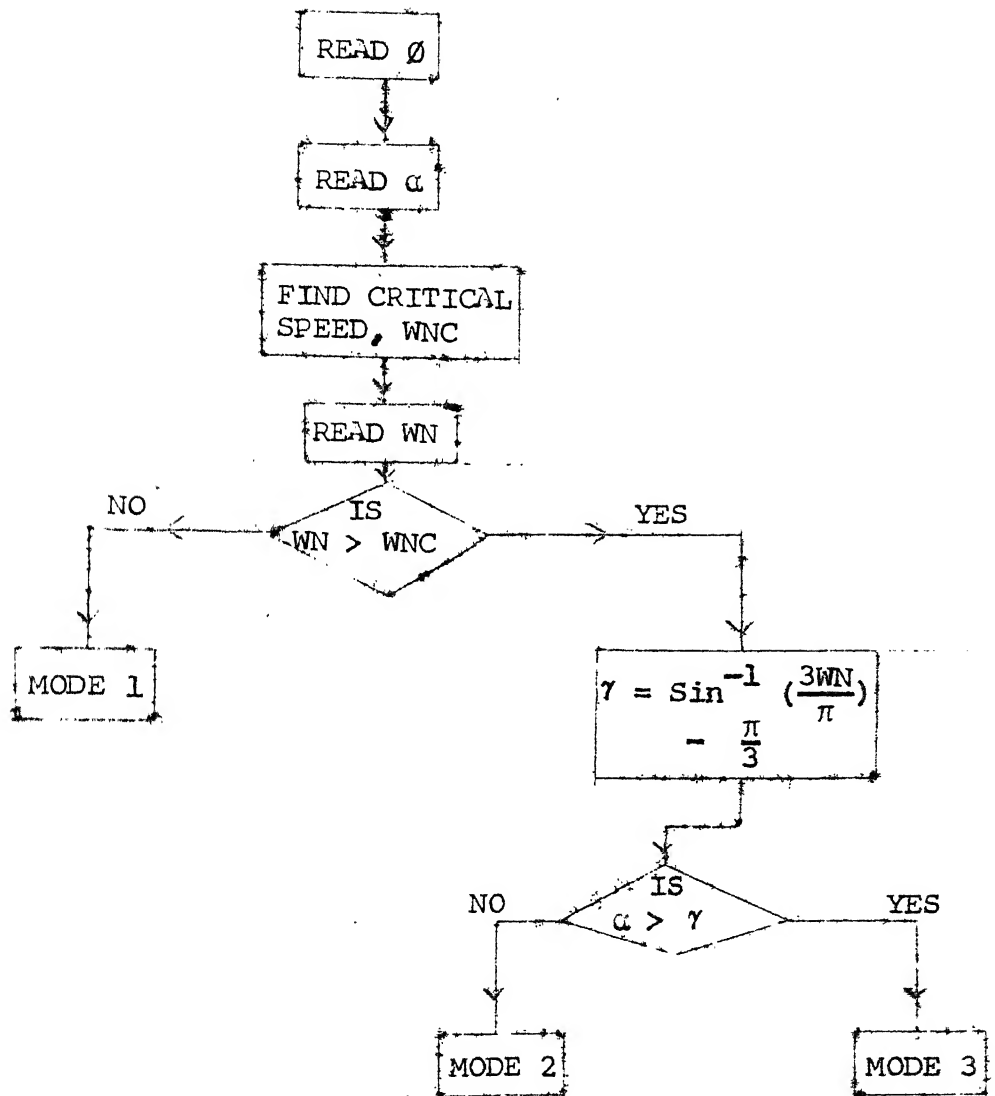


Fig. 3.5(a): Flow chart to identify the mode of operation for full controlled operation.

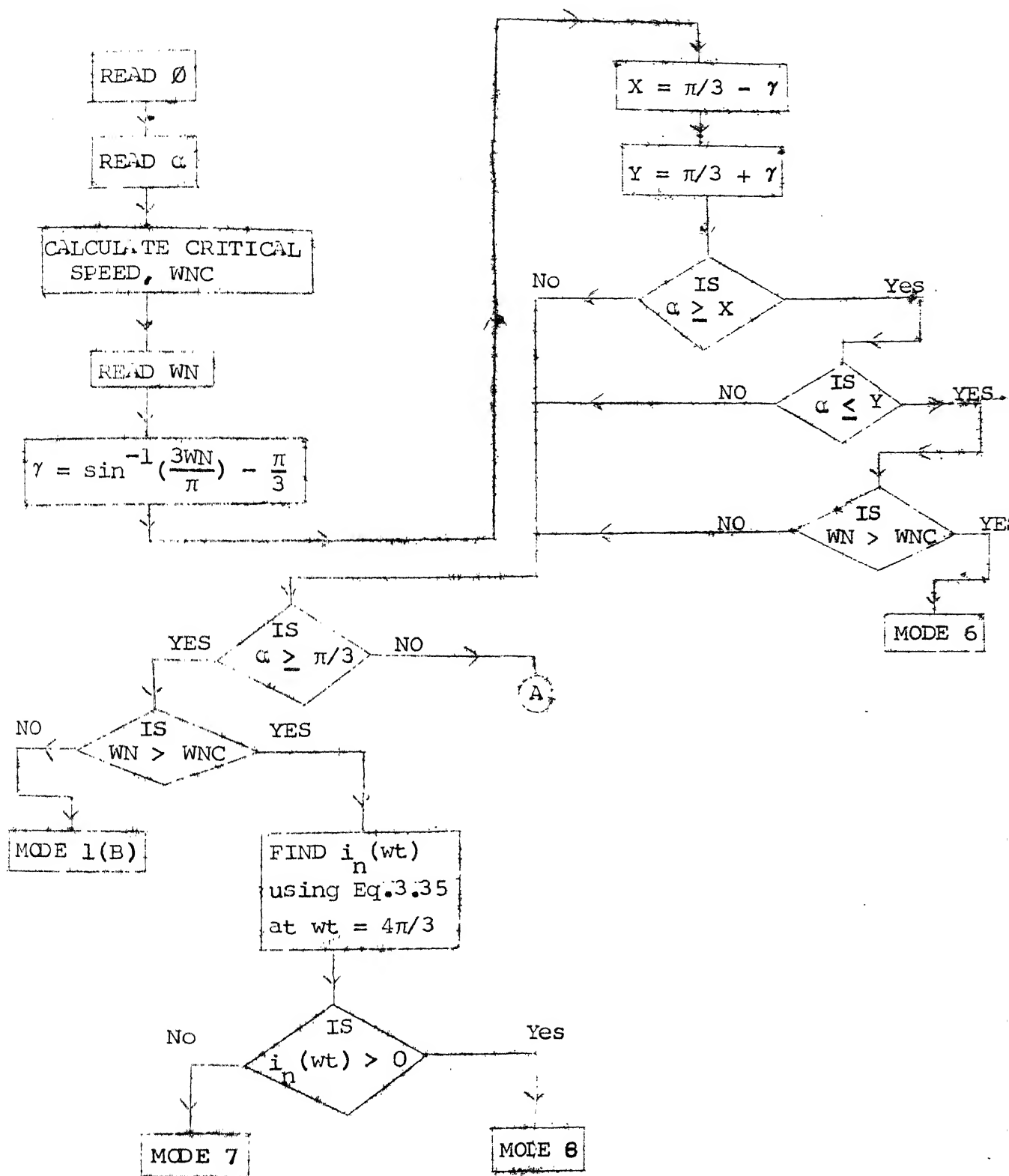


Fig. 3.5(b) (Continued)

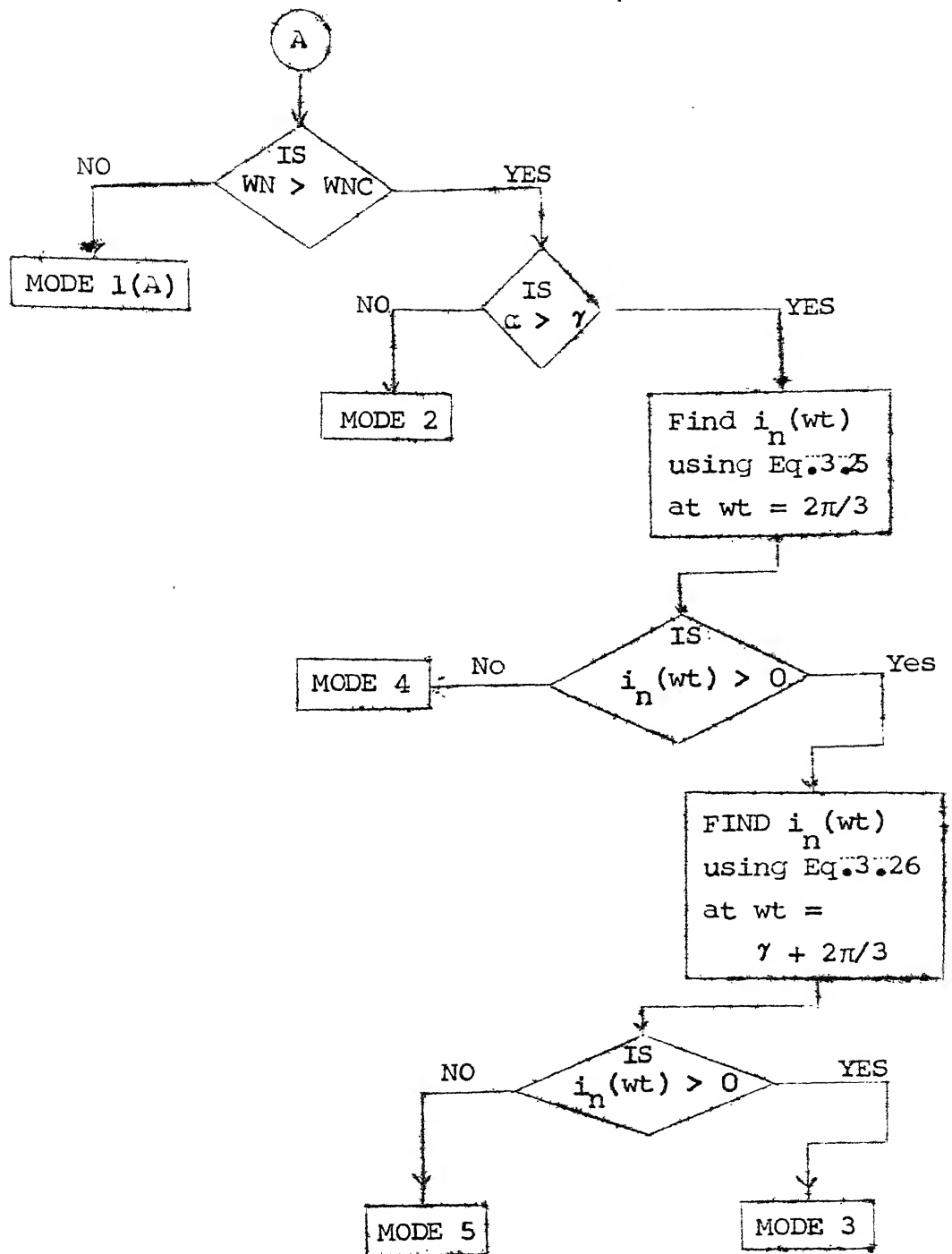


Fig. 3.5(b): Flow chart for identification of mode under half controlled operation.

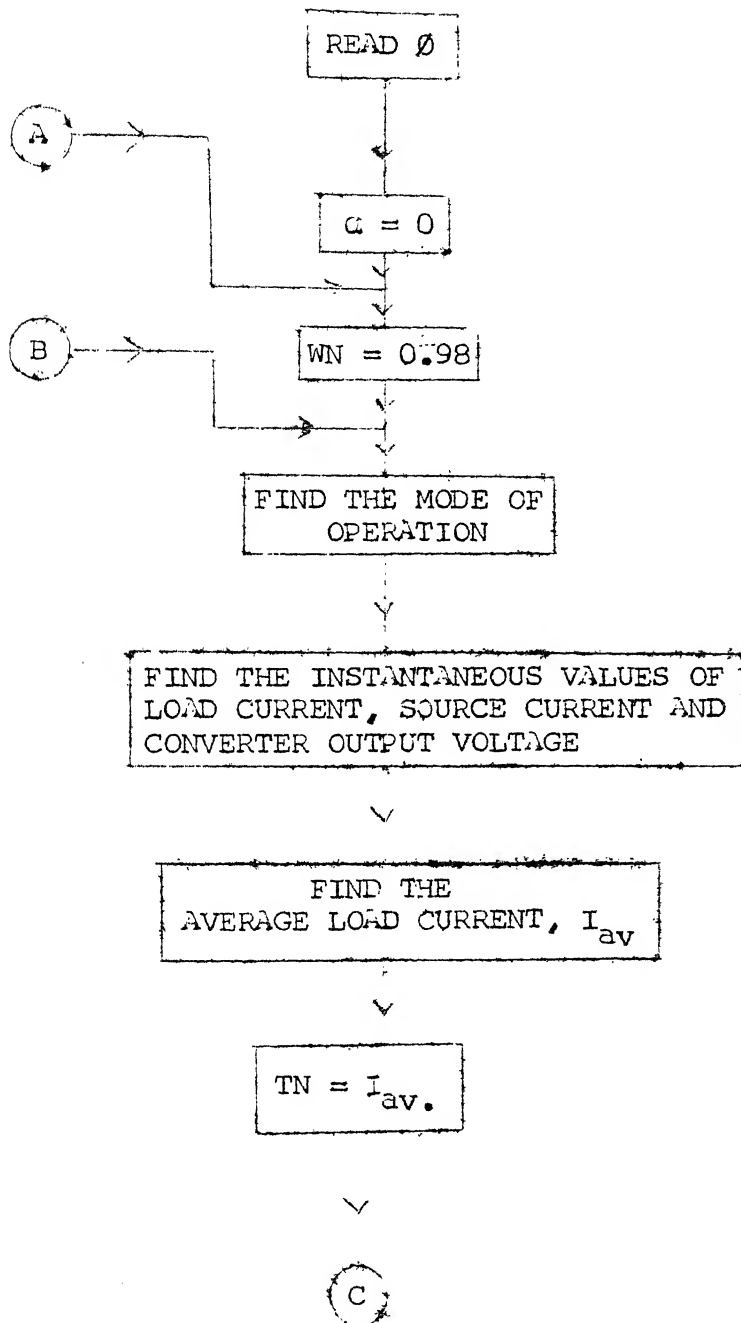
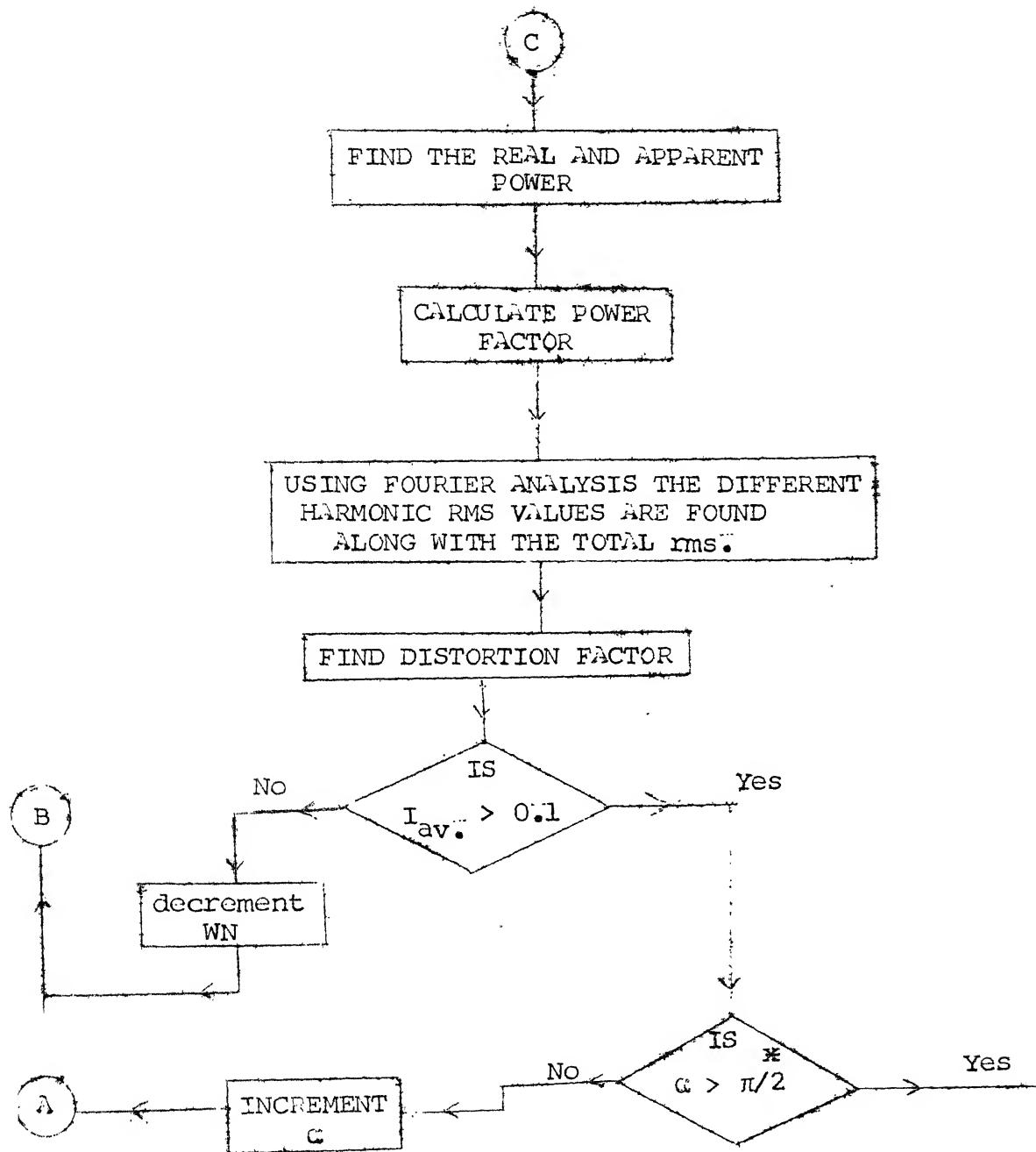


Fig. 3.6 (Continued)



* $\pi/2$ for full controlled operation
and π for half controlled operation.

Fig. 3.6: Flow chart to find TN, Power-factor, Distortion factor and harmonic contents.

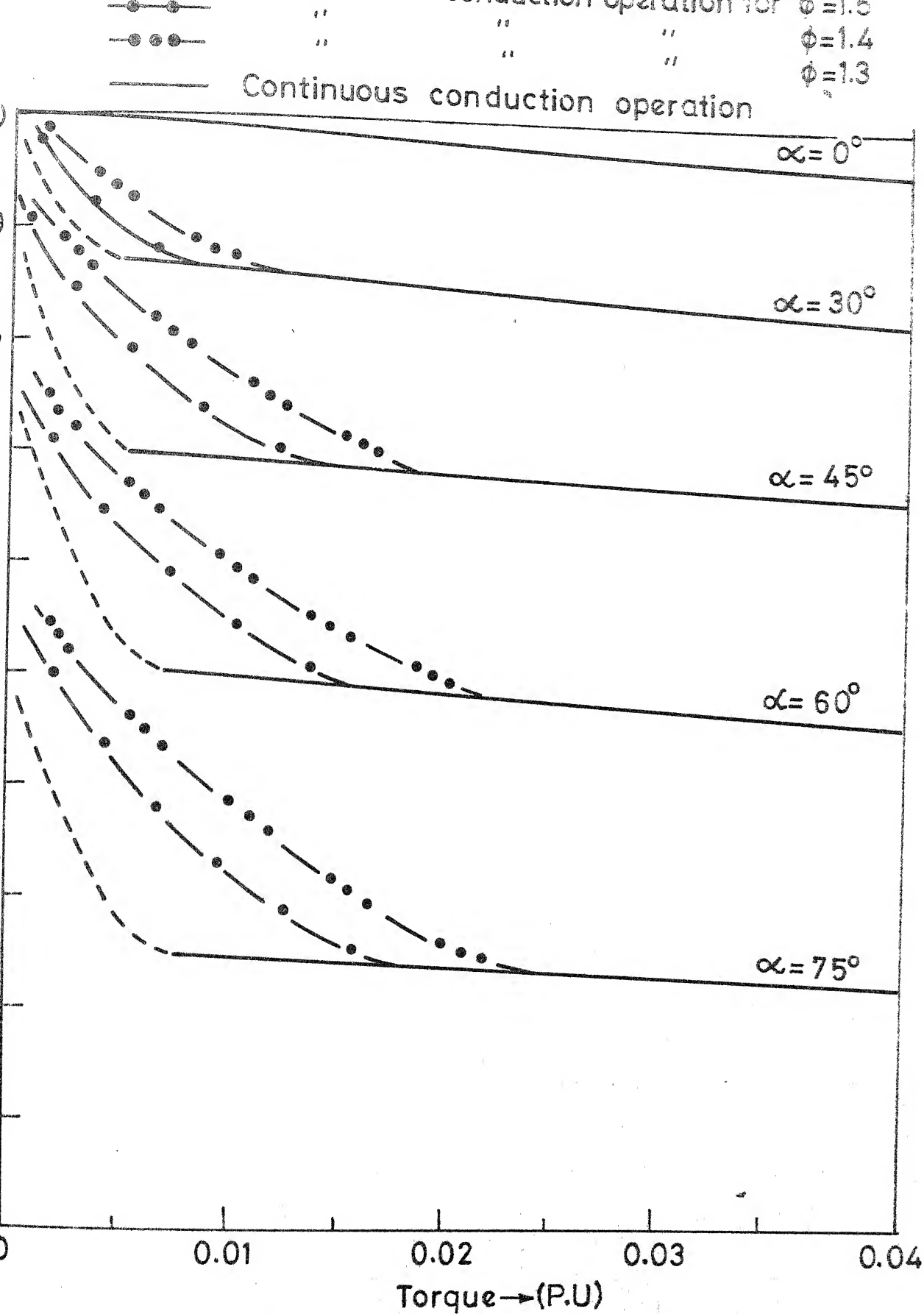


FIG.3.7(a) SPEED-TORQUE CHARACTERISTICS FOR SIX-PULSE
 CONVERTER FED DC SEPERATELY EXCITED MOTOR

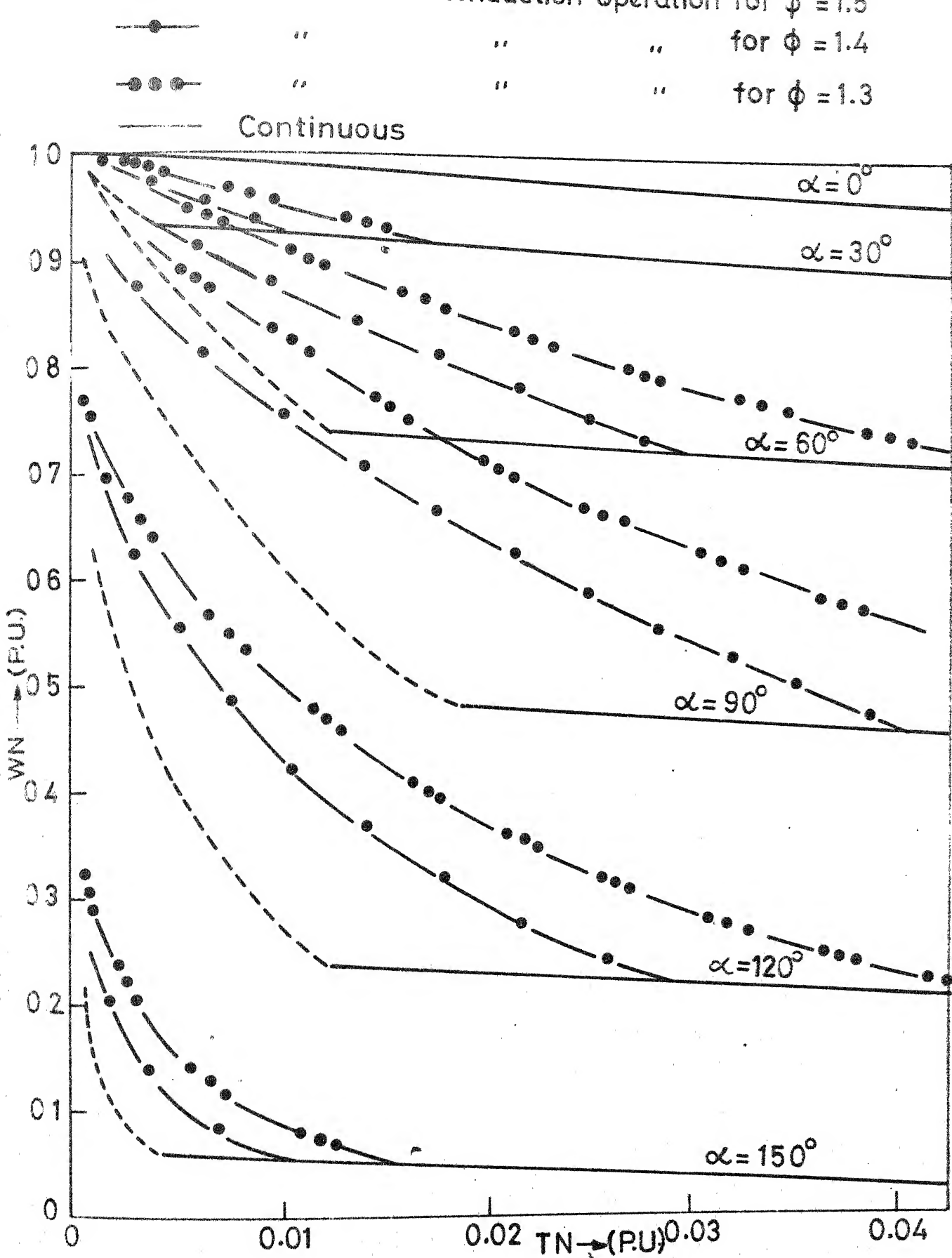


FIG.3.7(b) SPEED-TORQUE CHARACTERISTICS FOR HALF CONTROLLED OPERATION

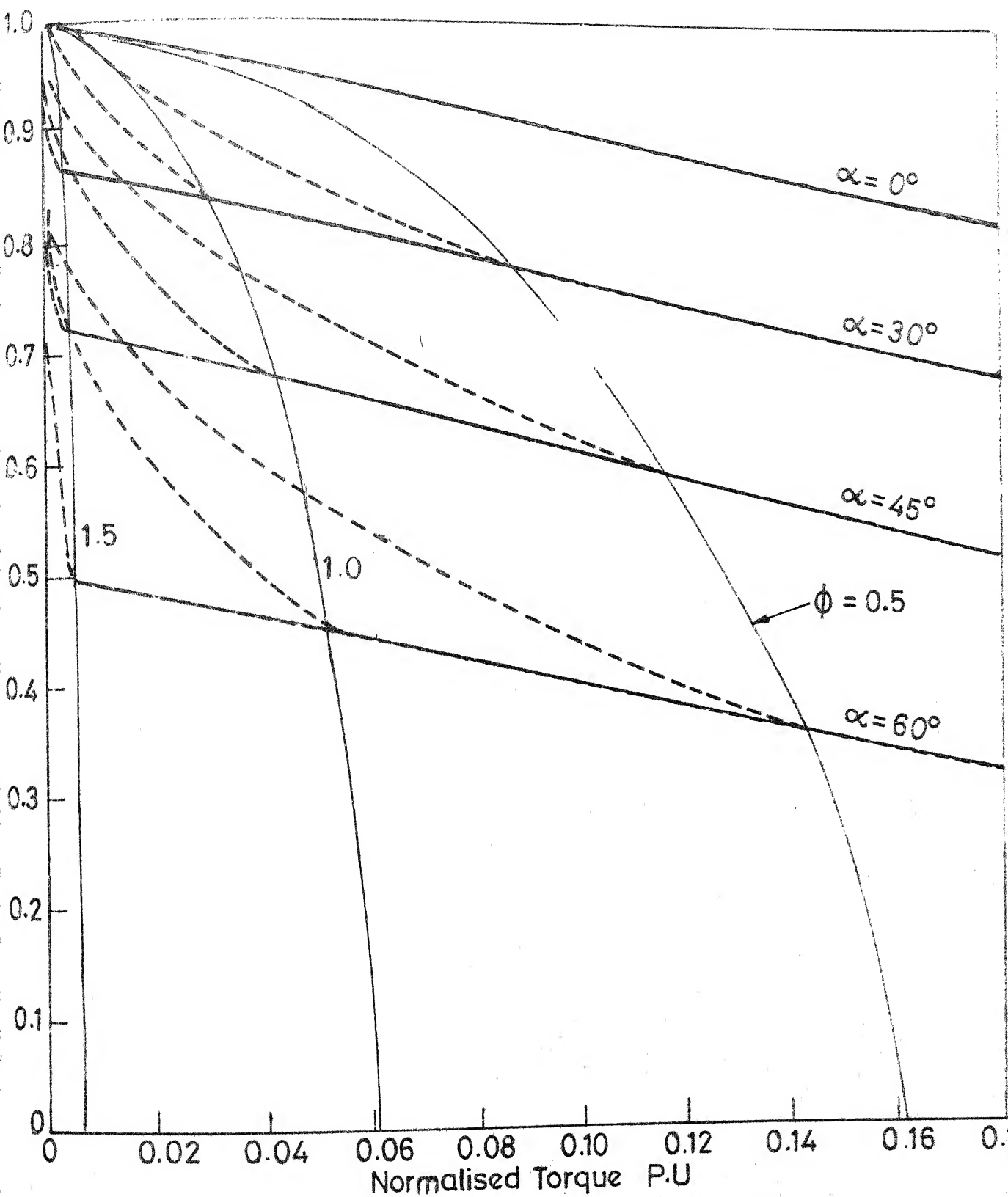


FIG.3.7(c) S-T CHARACTERISTICS UNDER FULLY CONTROLLED OPERATION

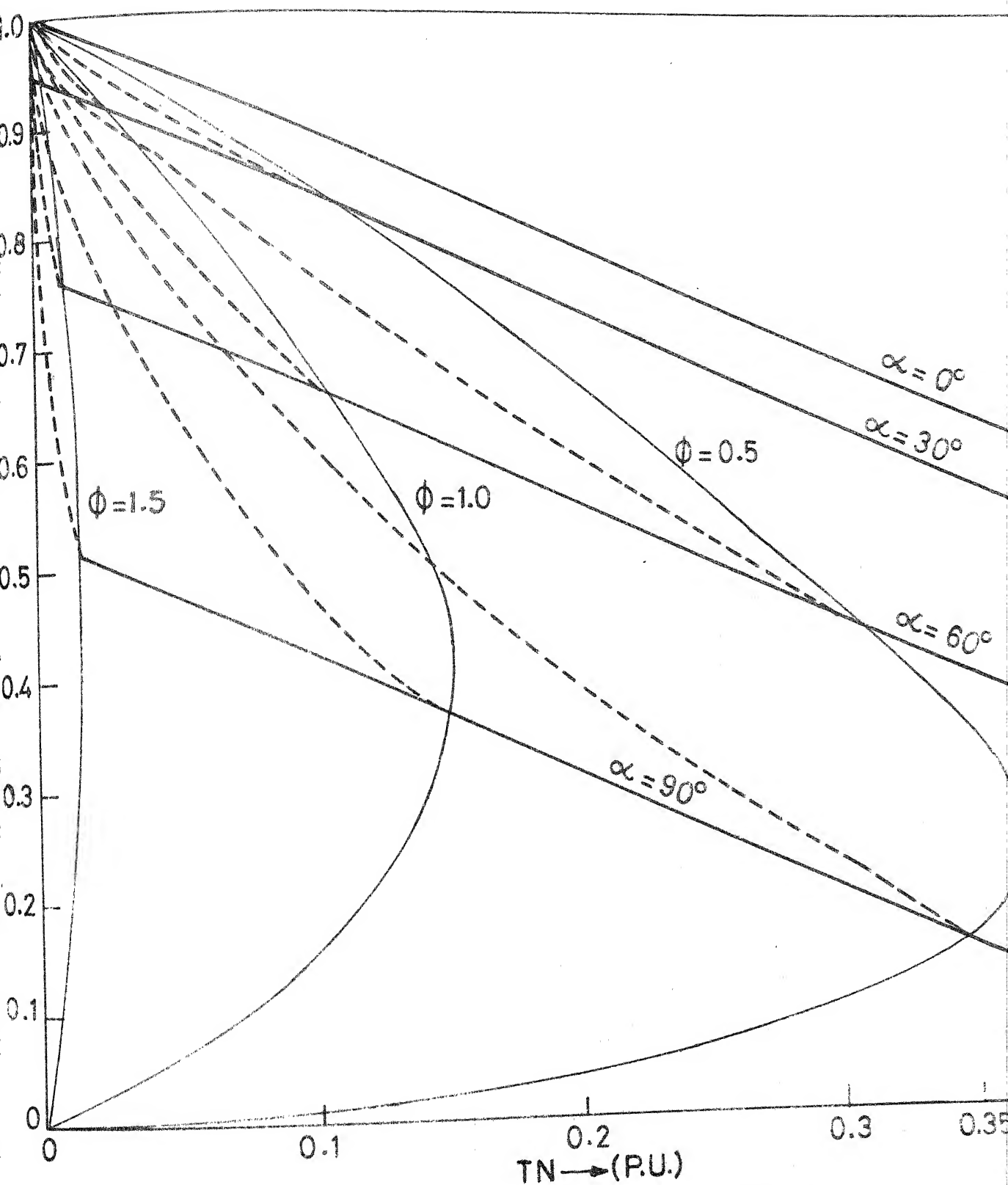


FIG.3.7(d) SPEED-TORQUE CHARACTERISTICS UNDER HALF CONTROLLED OPERATION

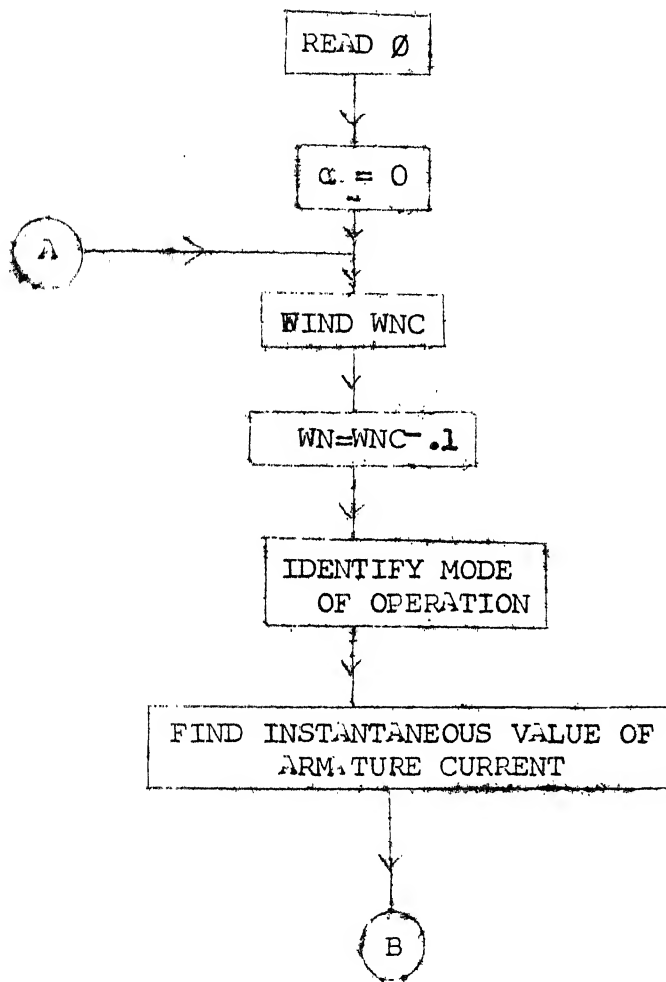
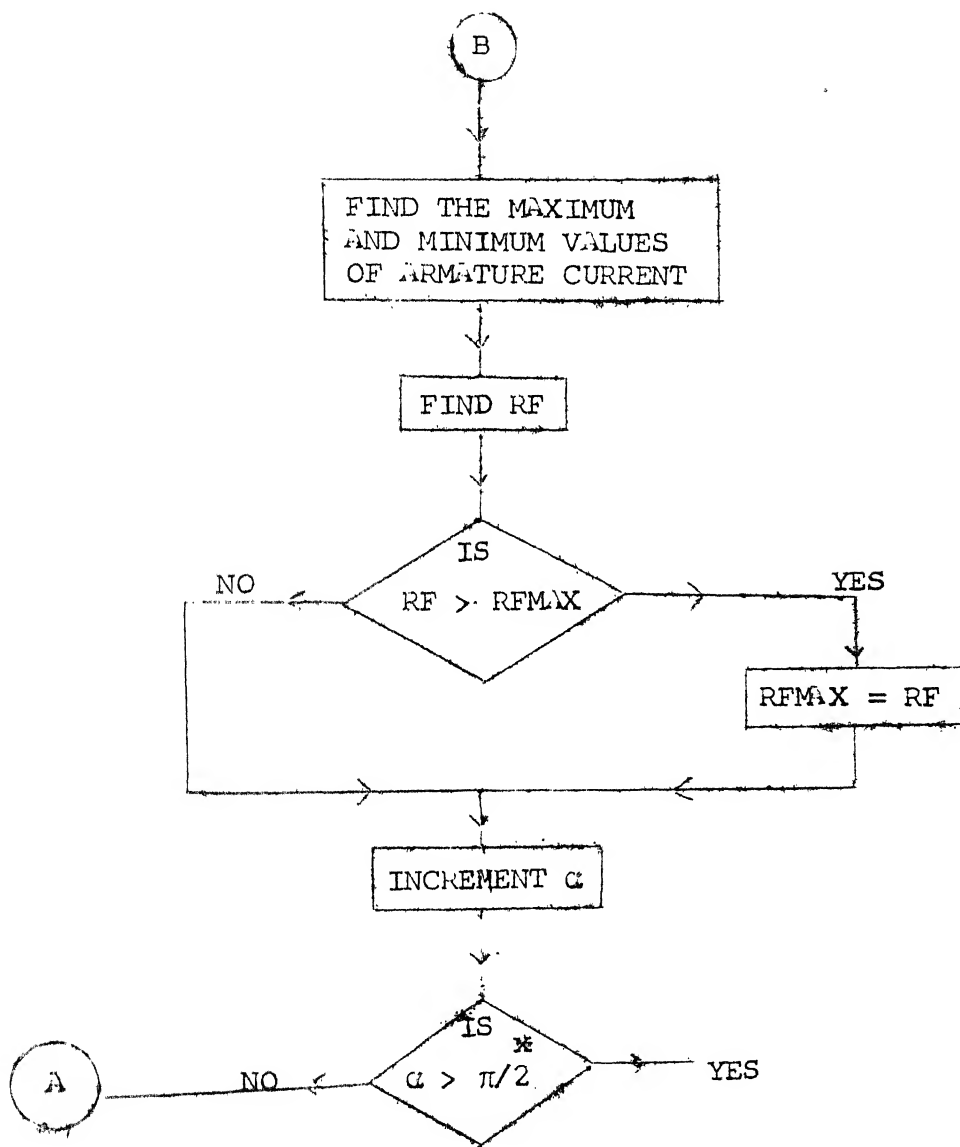


Fig. 3.8 (Continued)



* $\pi/2$ for full controlled operation

π for half controlled operation

Fig. 3.8: Flow chart for finding the maximum ripple factor for a given ϕ .

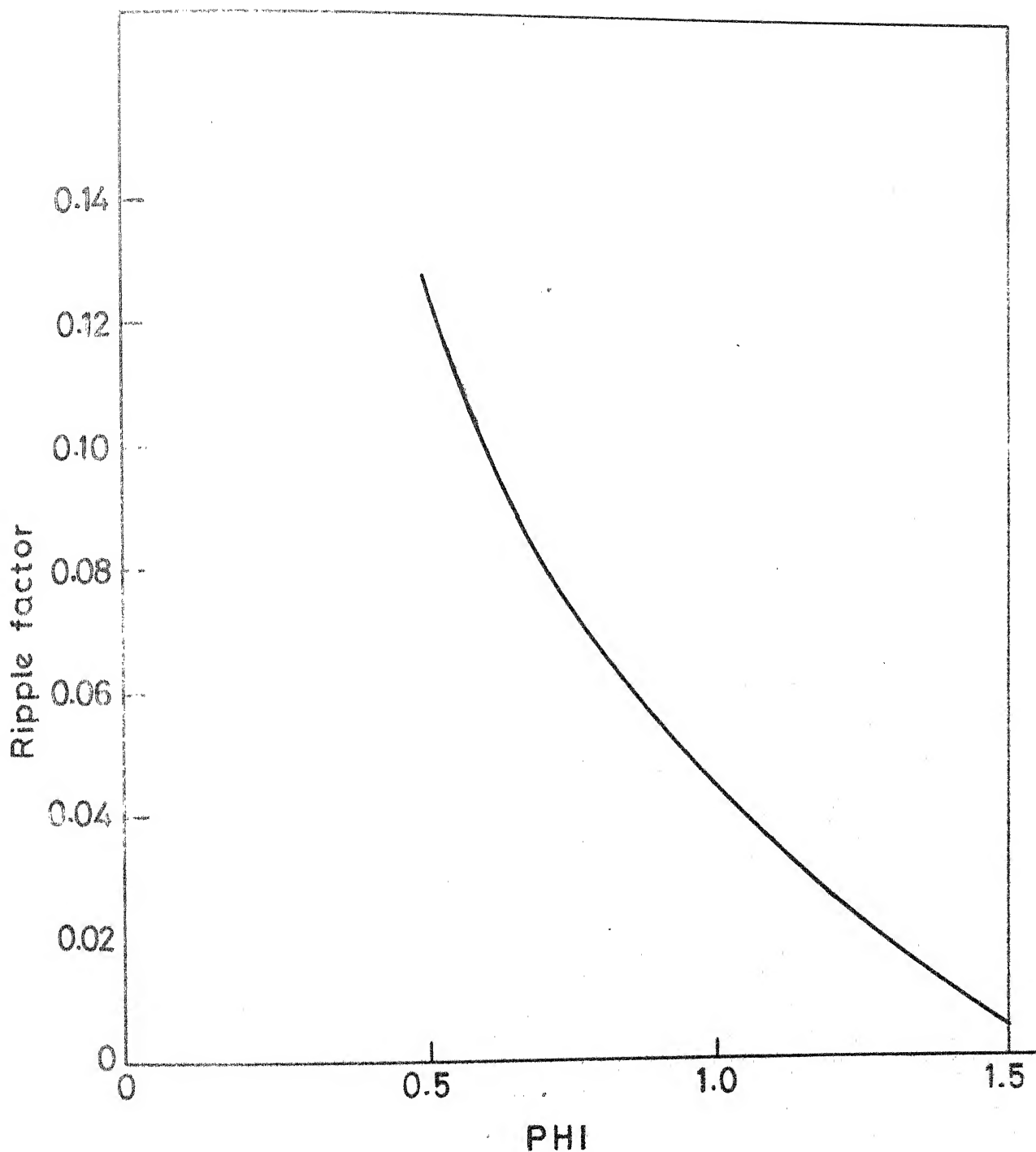


FIG.3.9(a) MAXIMUM R F VARIATION FOR DIFFERENT PHASE ANGLE VALUES UNDER FULLY CONTROLLED OPERATION

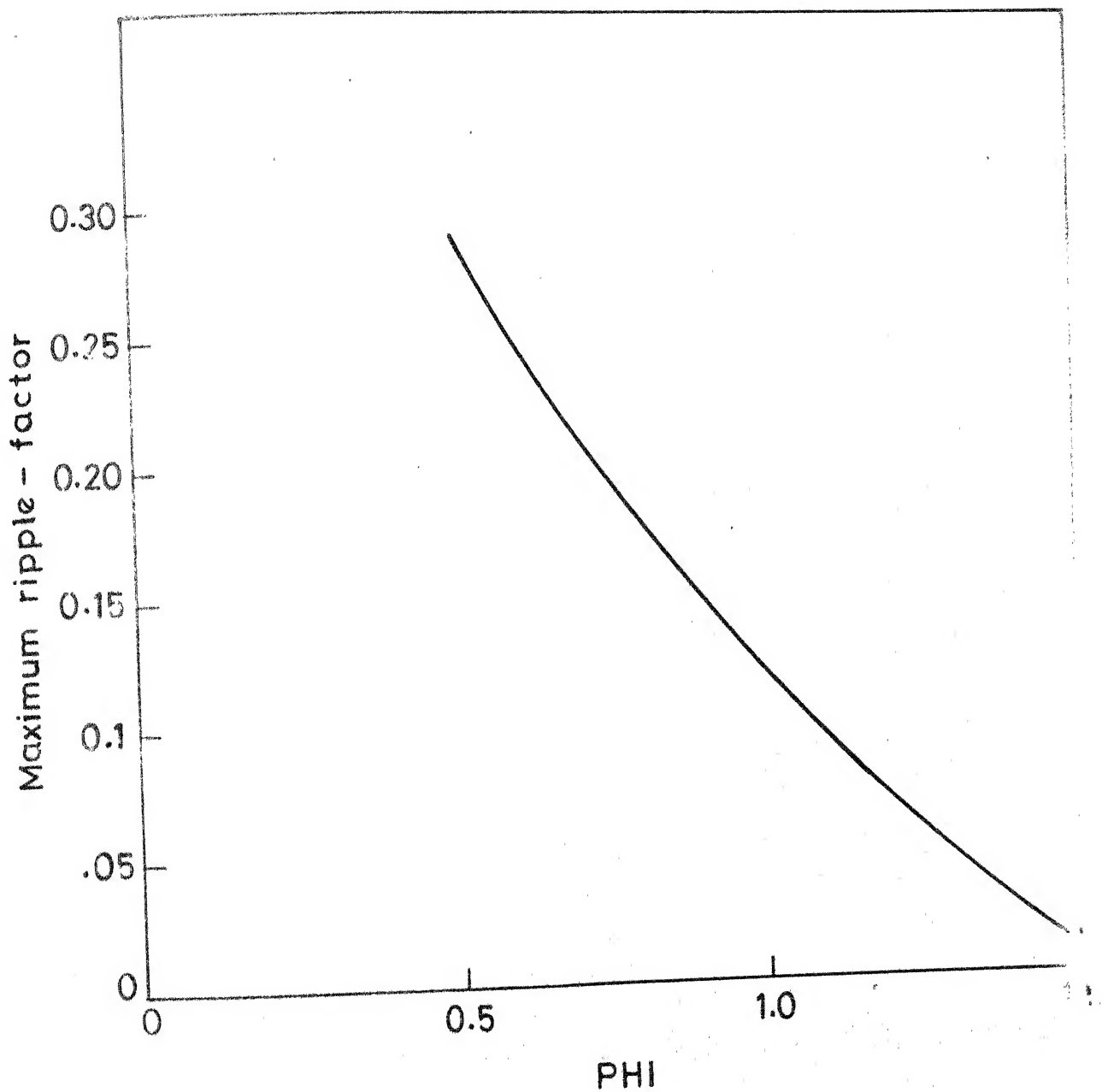


FIG.3.9(b) MAXIMUM RIPPLE FACTOR VARIATION FOR DIFFERENT PHASE ANGLE VALUES UNDER HALF CONTROLLED OPERATION

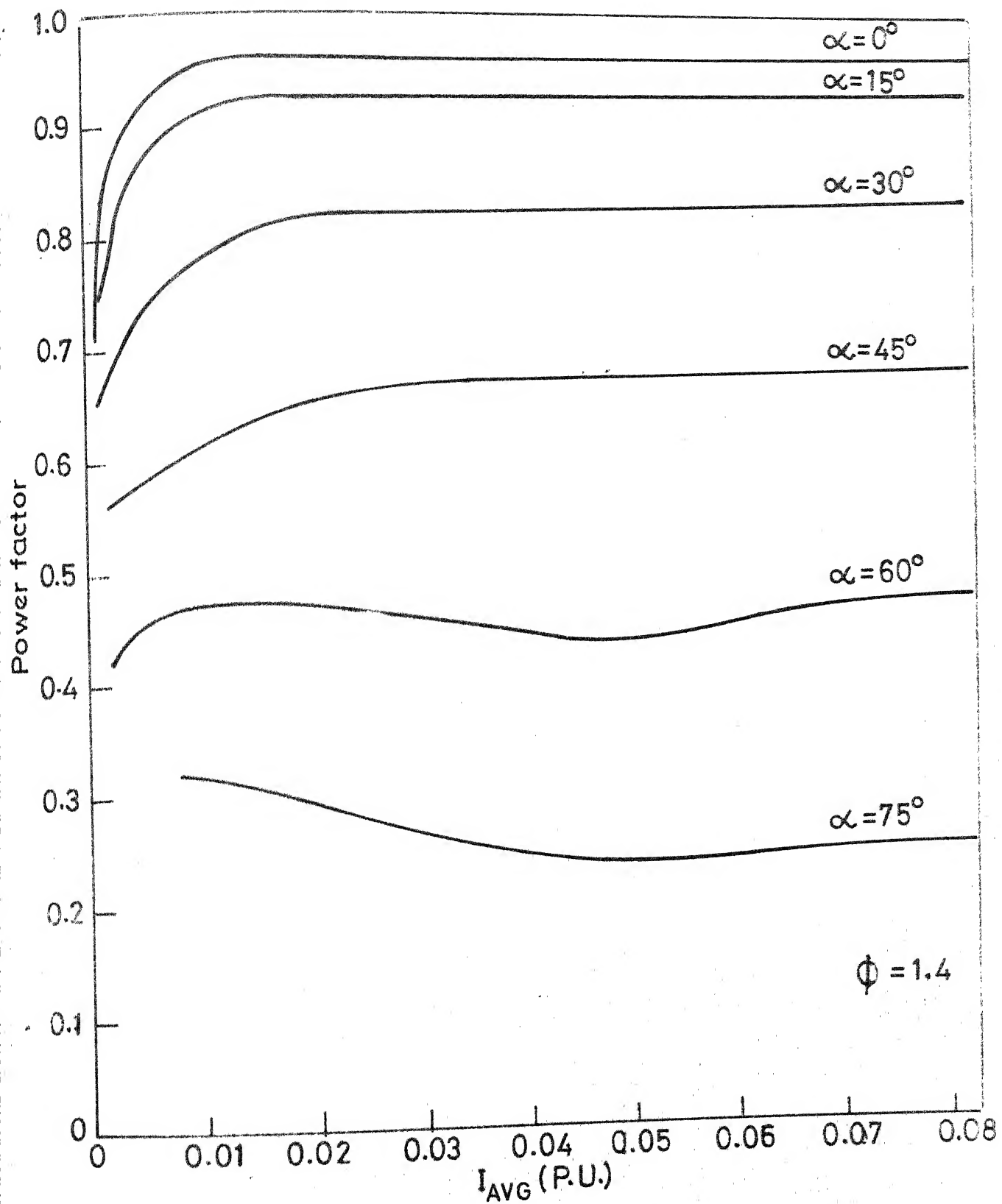


FIG.3.10(a) POWER FACTOR VARIATION WITH AVERAGE LOAD CURRENT FOR FULLY CONTROLLED OPERATION

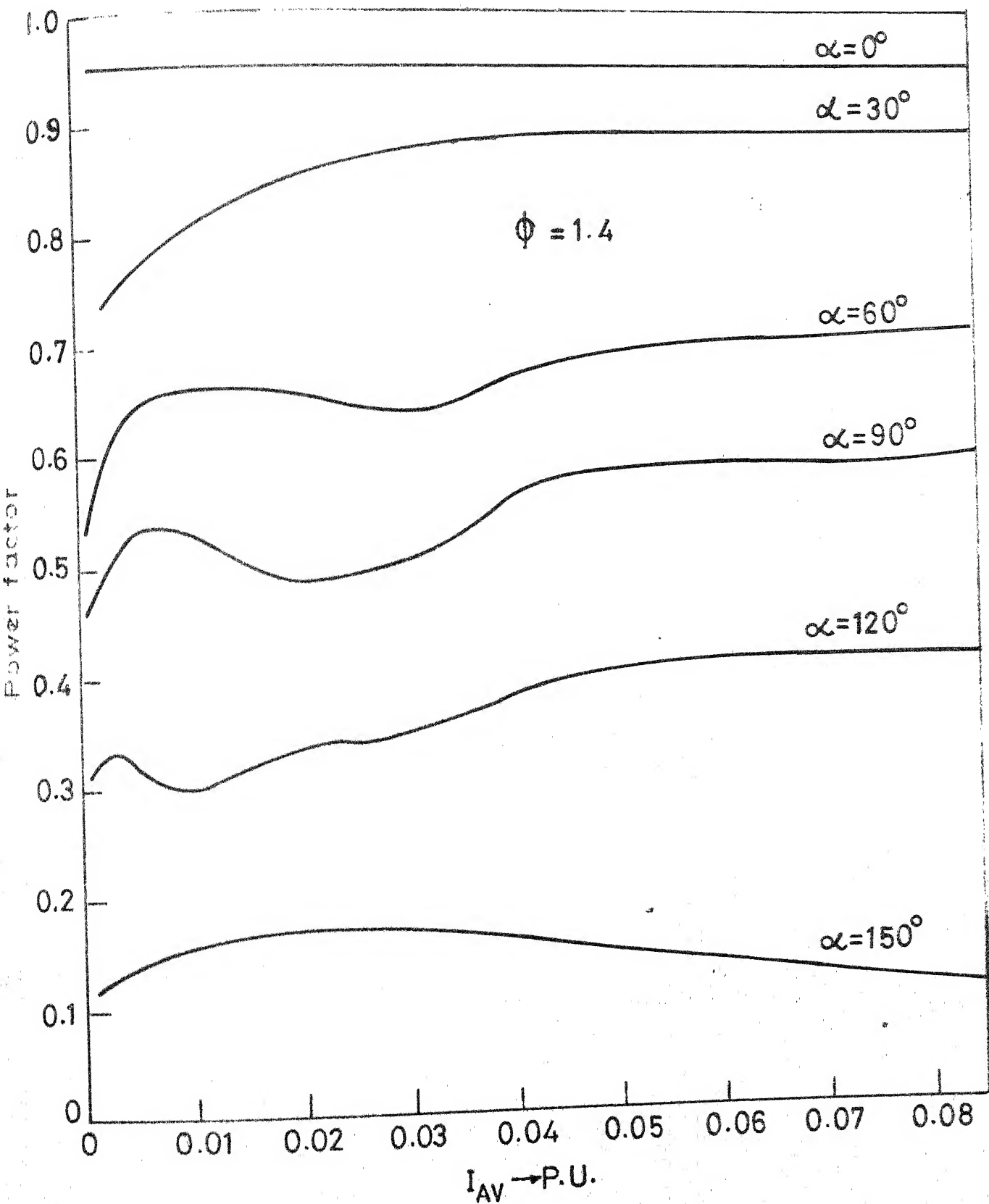


FIG. 3.10(b) POWER FACTOR VARIATION WITH AVERAGE LOAD CURRENT FOR HALF CONTROLLED OPERATION

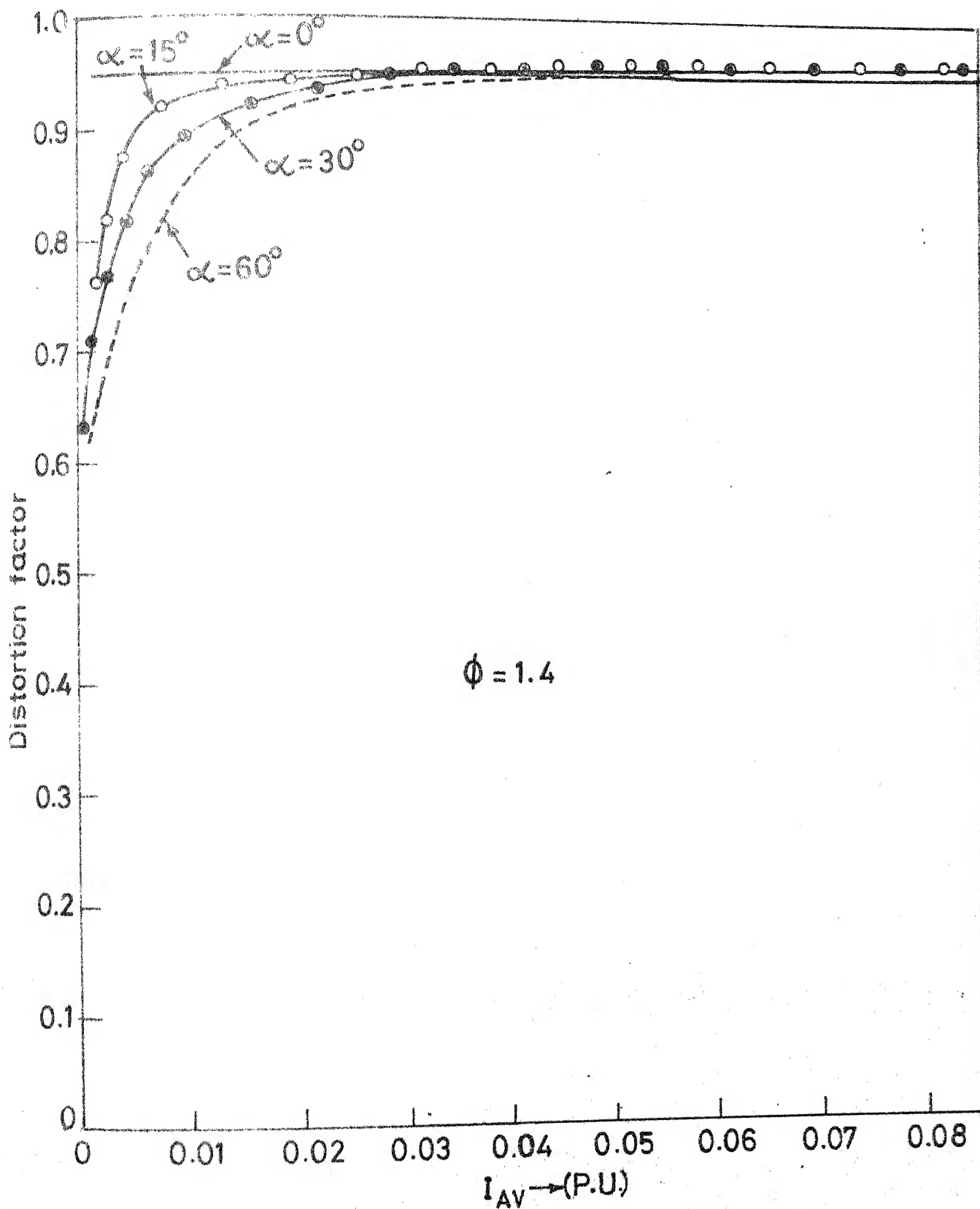


FIG.3.11(a) DISTORTION FACTOR VARIATION WITH AVERAGE LOAD CURRENT-FULLY CONTROLLED OPERATION

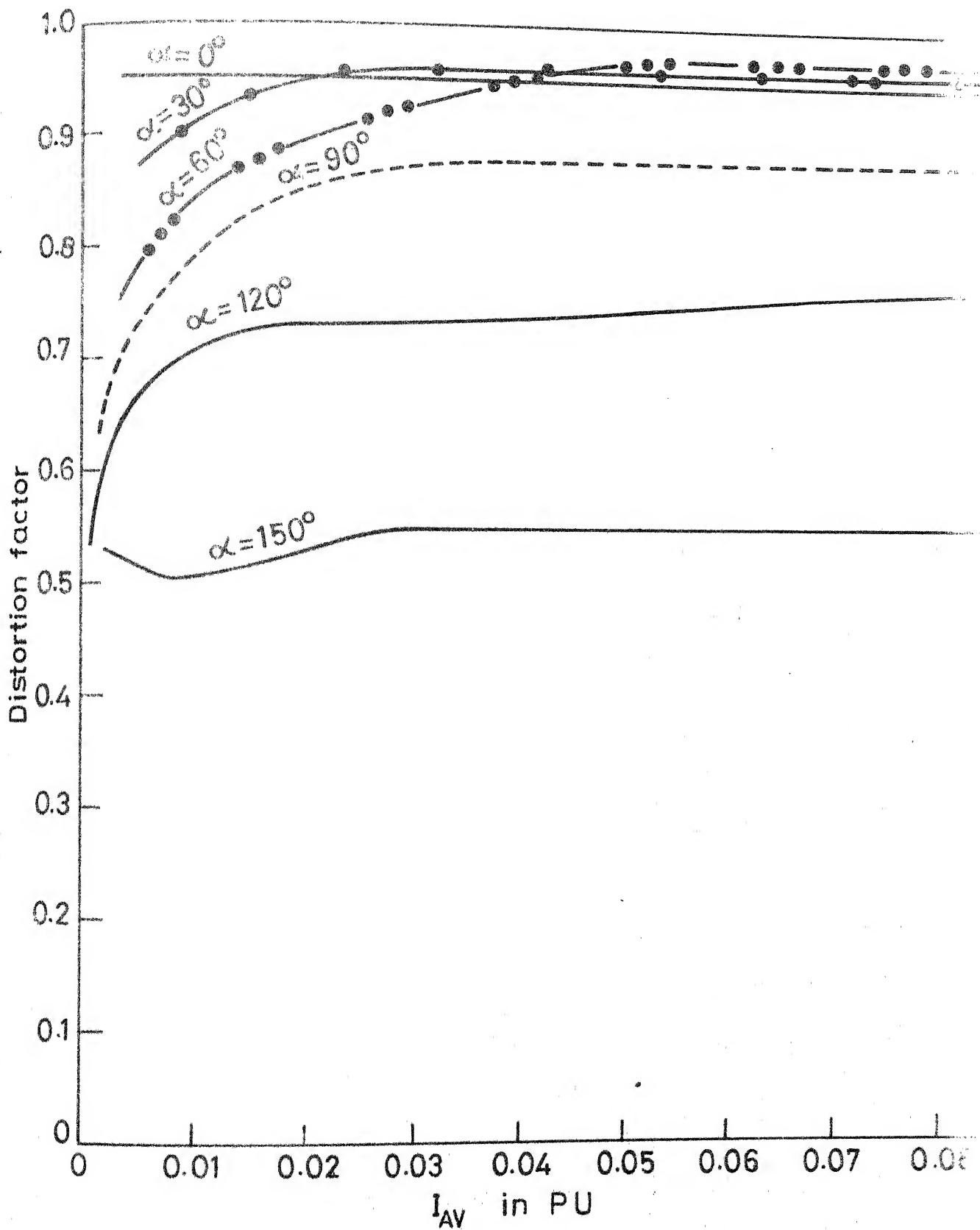


FIG.3.11(b) DISTORTION FACTOR VARIATION WITH LOAD CURRENT FOR HALF CONTROLLED OPERATION

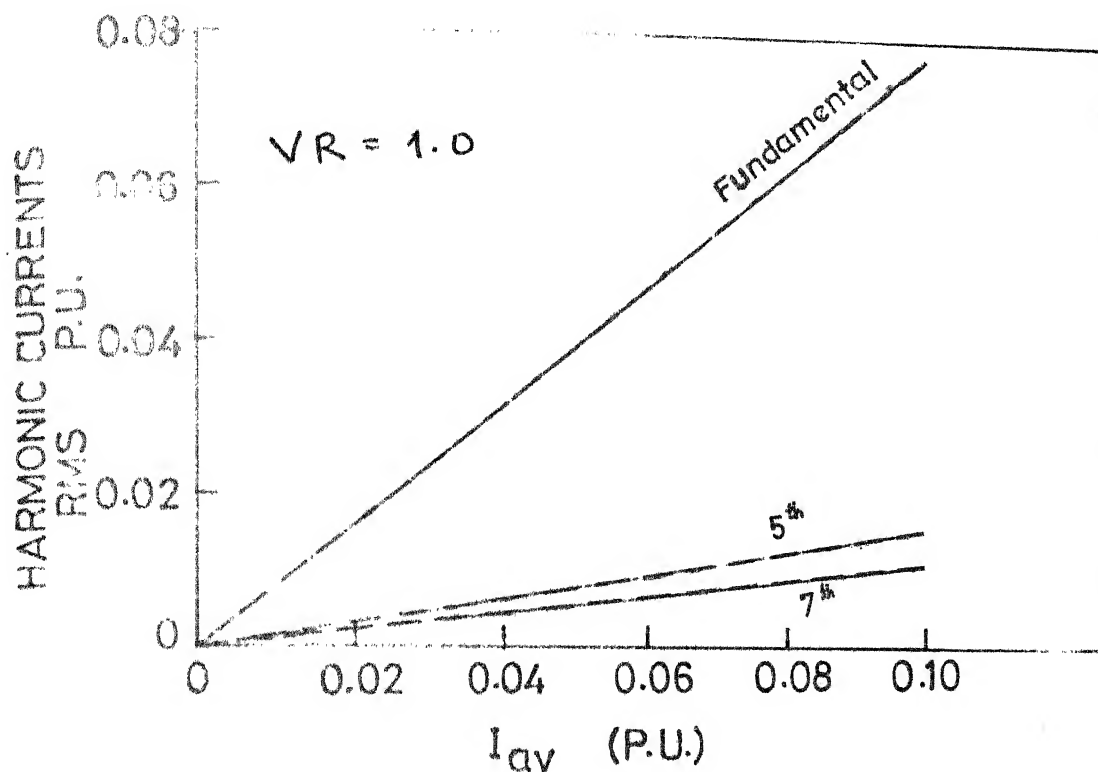


FIG.3.12 (a)

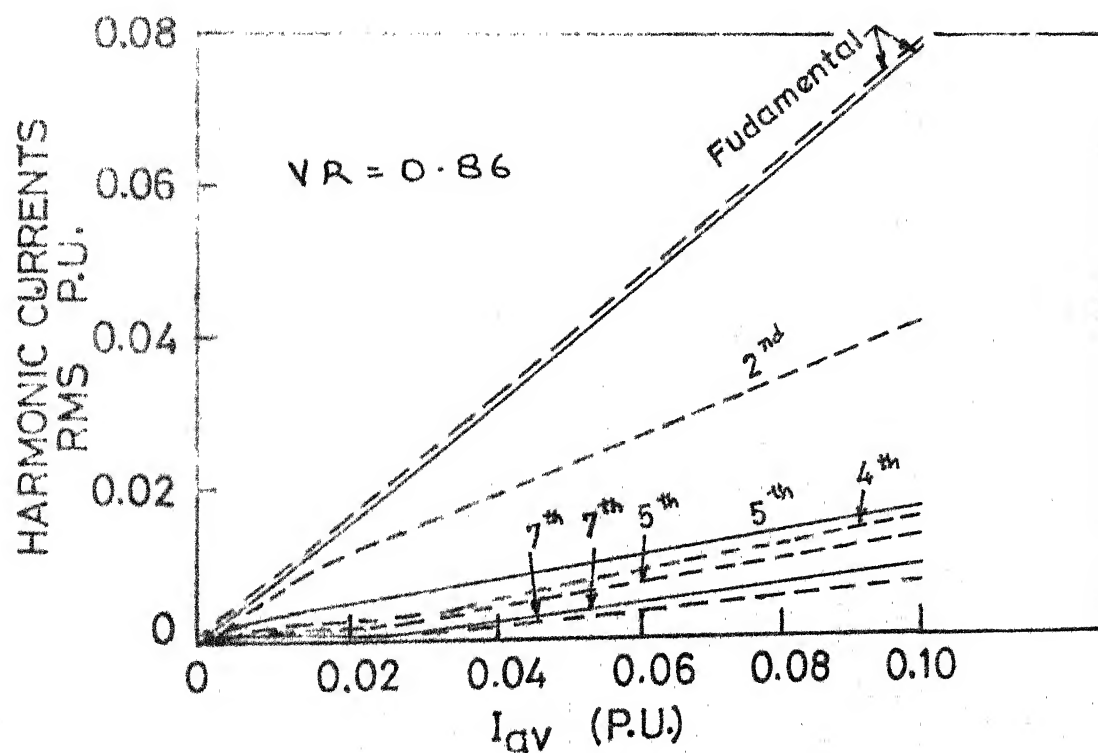


FIG.3.12(b) HARMONIC CONTENTS IN SOURCE CURRENT
(continued)

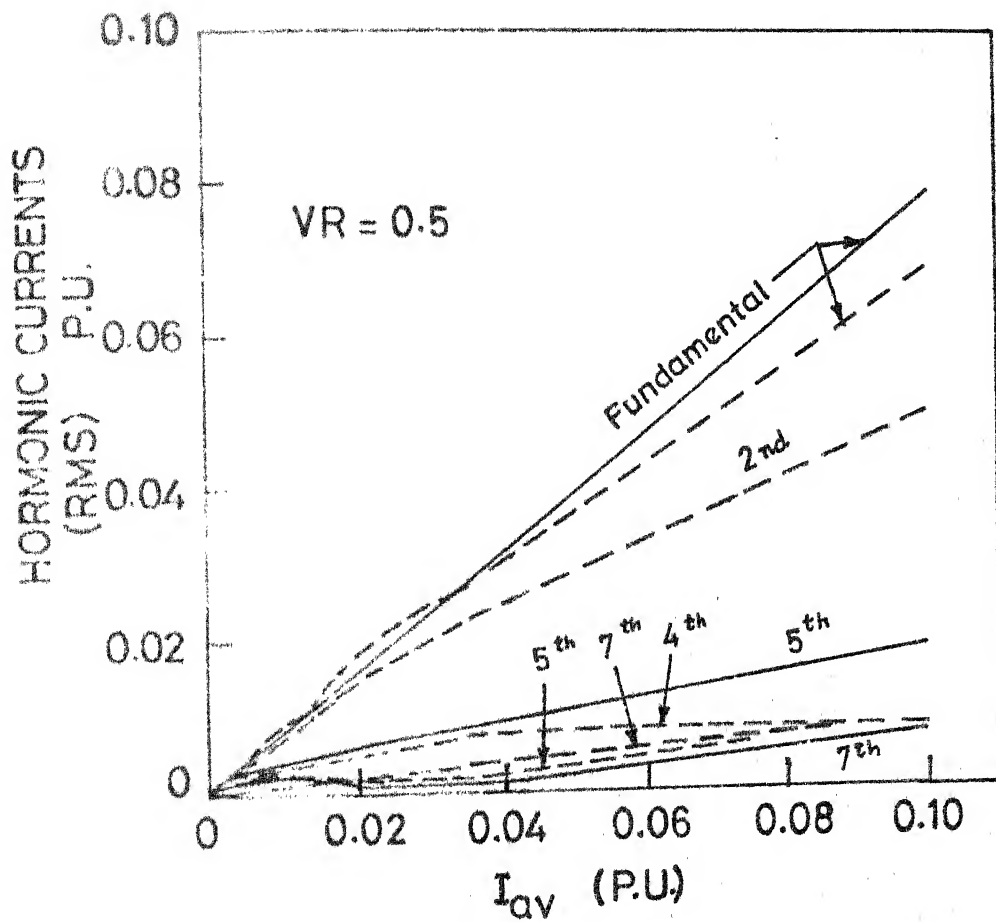


FIG.3.12(c)

----- HALF CONTROLLED OPERATION
 ——— FULL " "

CHAPTER IV

EXPERIMENTAL INVESTIGATION

4.1 THE FIRING CIRCUIT (for 3- ϕ converter)

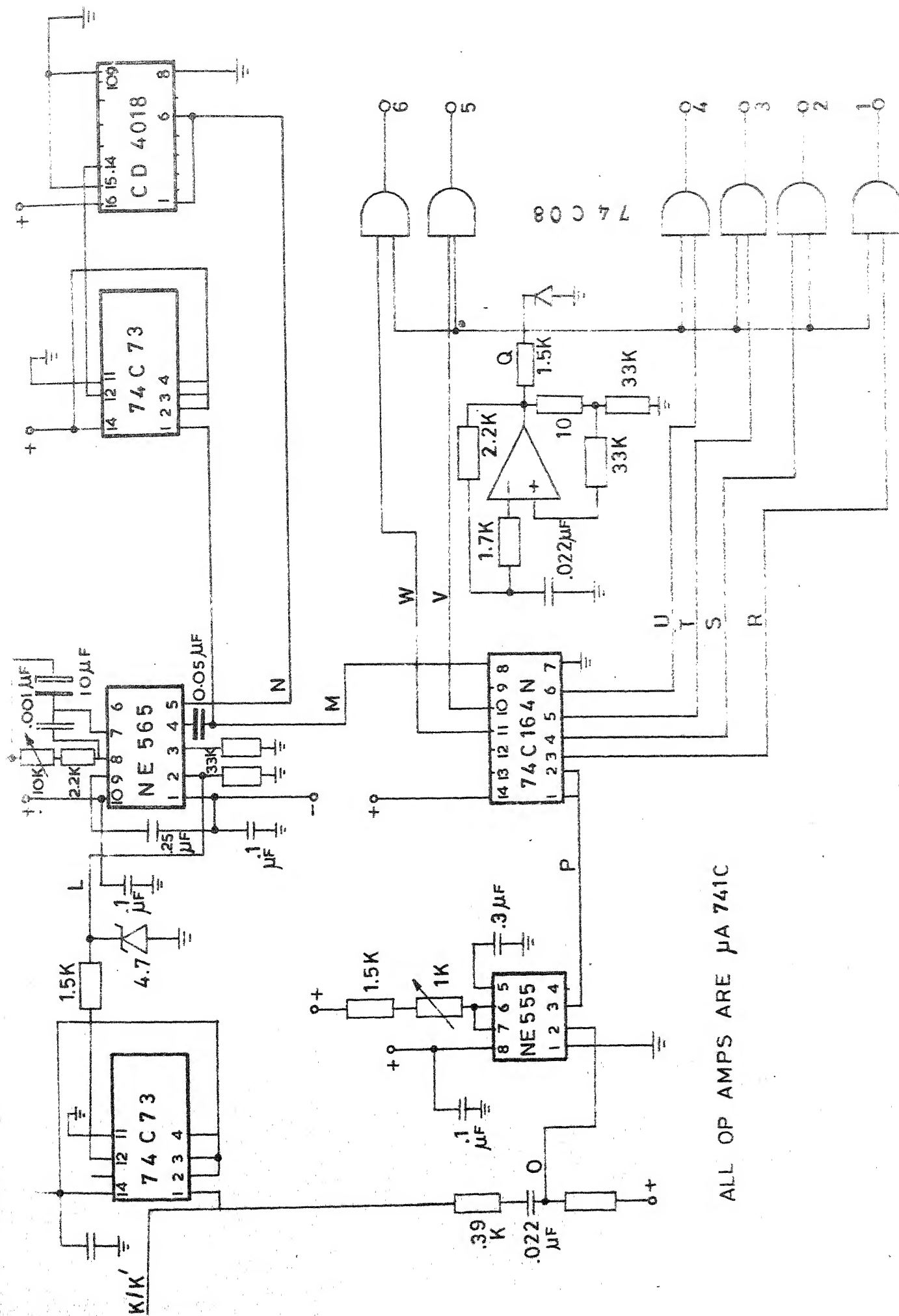
The firing circuit has been developed for both open and closed loop operation. It can be used in the closed loop scheme for half and full controlled operation. The firing scheme is built such that the output voltage of the converter, under continuous current operation, will be directly proportional to the control voltage.

The block diagram of the firing scheme is shown in Fig. 4.1. The corresponding circuit diagram is shown in Fig. 4.2. The waveforms at the various stages are shown in Fig. 4.3. The principle of operation is described below.

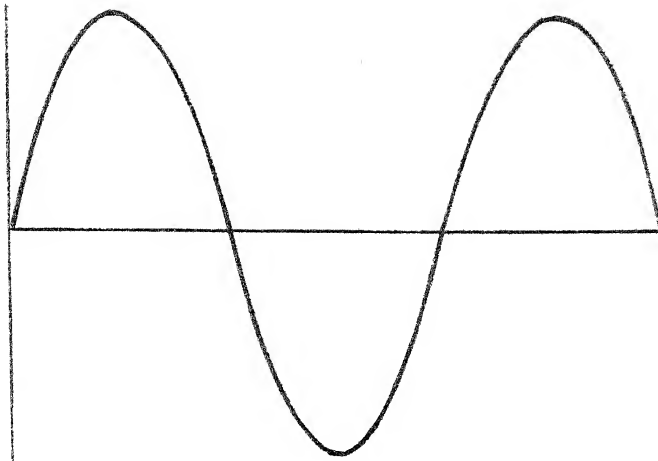
The synchronising input A is integrated to get a cosine wave B. This cosine wave is added to pulses G and H to get a cosine wave saturated at the peaks. This avoids instability in case the input a.c. voltage decreases and α is near 0 or π . The resultant cosine wave I is level shifted to get waveform I' with $f(\alpha) = (1 + \cos \alpha)$. The wave I is compared with J to get the value of α for a fully controlled converter and I' is compared with J' to get α for a half controlled converter. The value of α thus obtained gives a converter output voltage proportional to the reference d.c. voltage.

A select switch is provided to select between half and fully-controlled operation. A high select input blocks the output of the comparator for half controlled operation and we get the output of the other comparator. A low select input on the other hand gives a for half controlled operation.

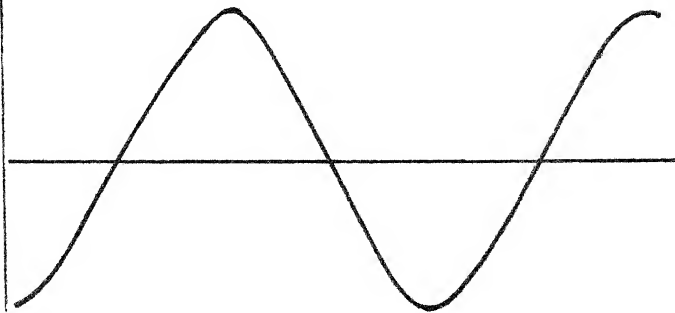
The comparator output K or K' triggers a JK so that the two half cycles are of equal width. The frequency of the output of the JK flip flop L, is half the supply frequency. L is fed as a synchronising input to a 'Phase Locked Loop'. The PLL has in its feed back path a 'divide by 12 N' counter. N is kept high to reduce phase errors. By having a 'divide by 12N' counter in the feed-back the output of the PLL has a frequency of $6Nf$. The PLL output is fed into a $\frac{1}{N}$ counter which is synchronised with L by resetting it with the help of a monostable. The output of the $\frac{1}{N}$ counter thus has a frequency of $6f$, synchronised with L as shown by M. L is again used to trigger a monostable which has a pulse width of approximately 5 ms shown by N. M is fed as the clock input and N as the serial input for a 8-bit shift register. By ensuring N to be of about 5 ms we have the outputs of the shift register to be of 120° pulse width and each shifted by 60° from the other.



ALL OP AMPS ARE μ A 741C



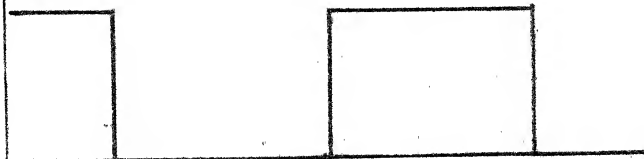
A



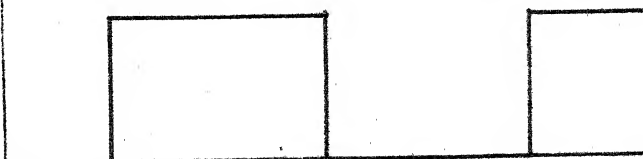
B



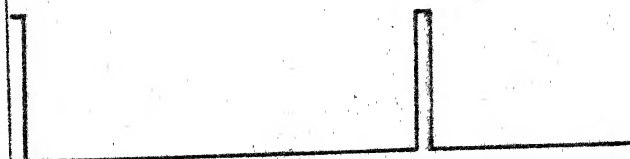
C



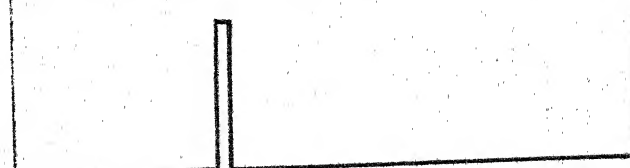
D



E



F



G

FIG. 4.3 (continued)

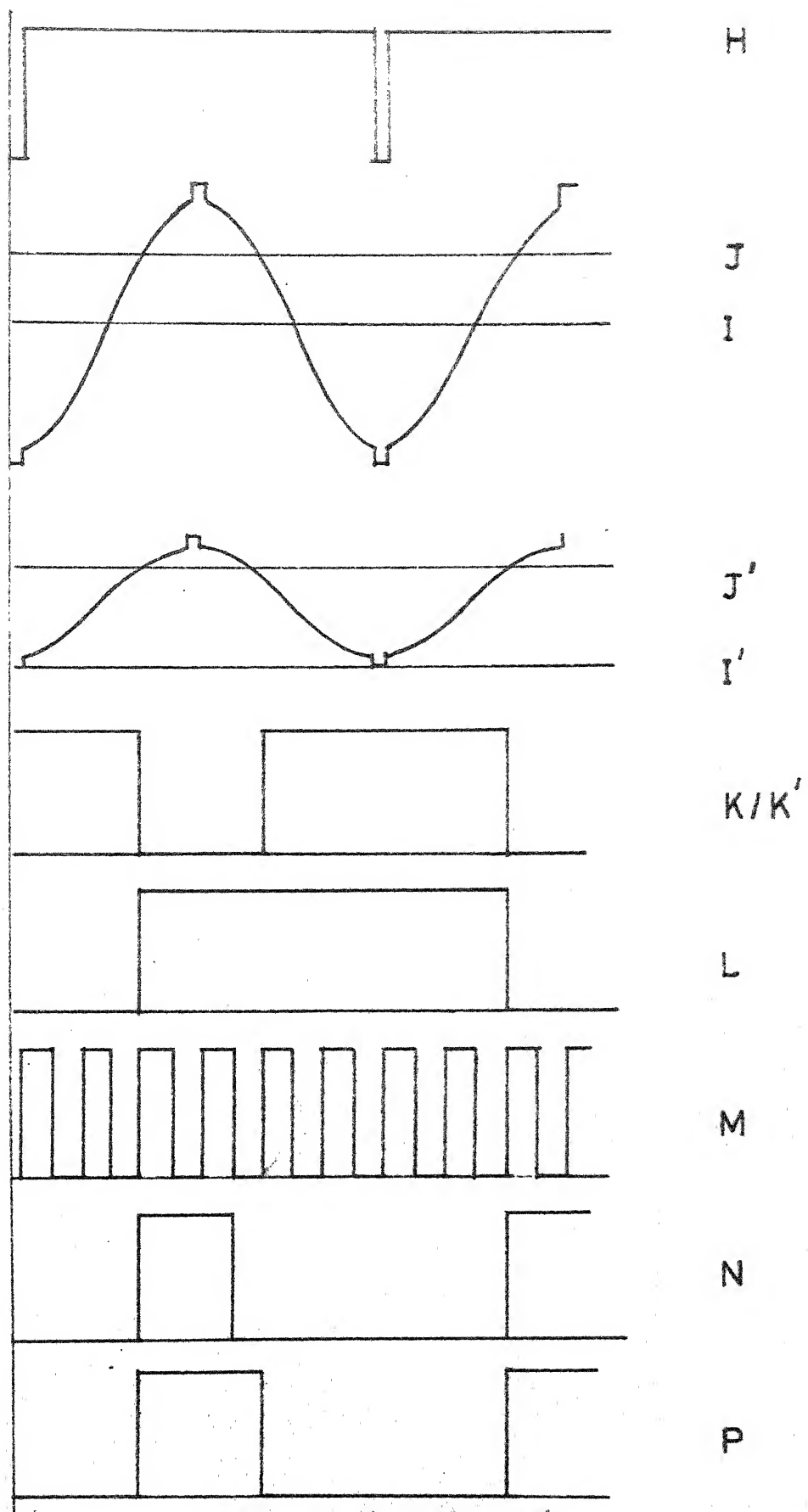


FIG.4.3 (continued)

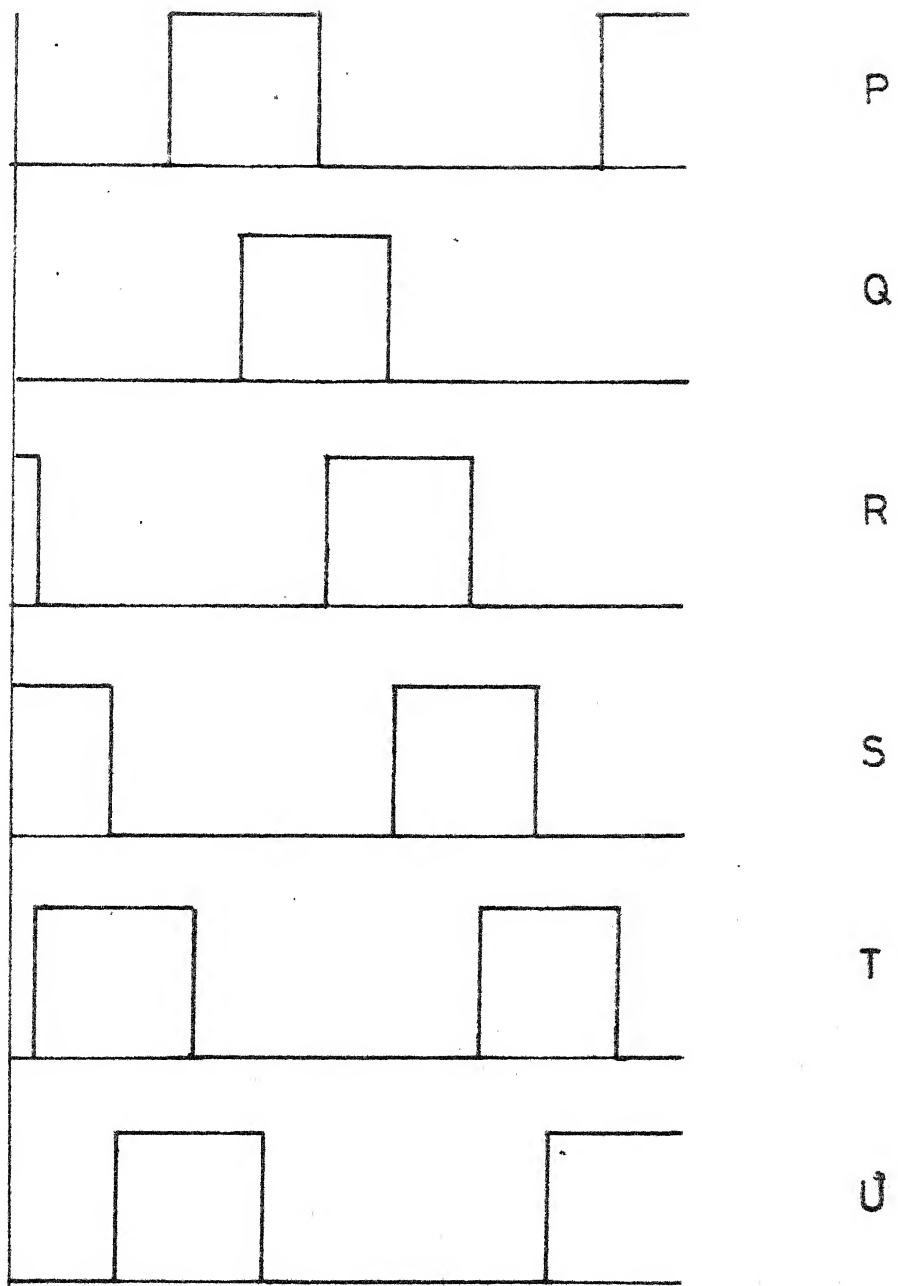


FIG. 4.3

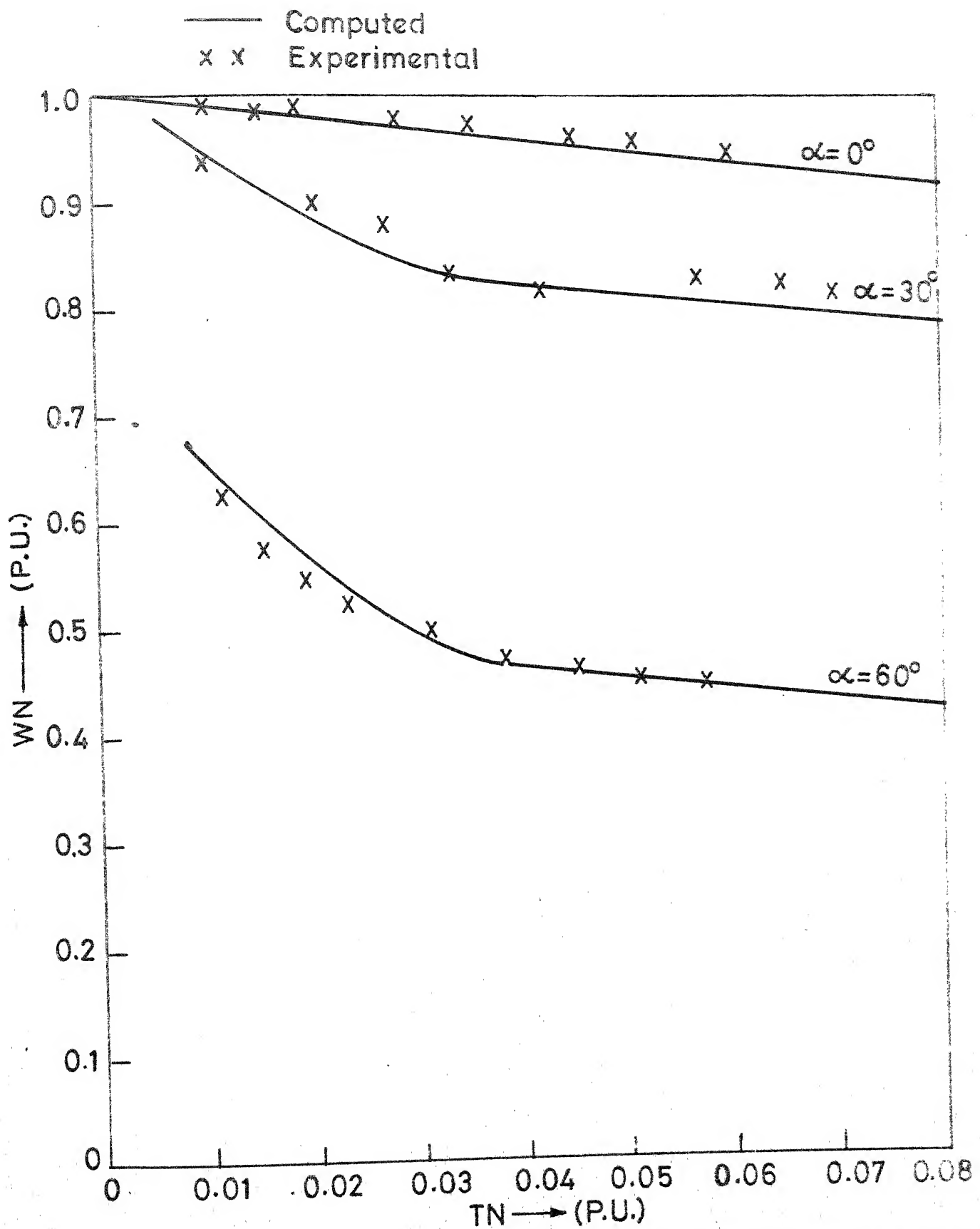


FIG. 4.4 EXPERIMENTAL VERIFICATION FOR SPEED-TORQUE CHARACTERISTICS FOR FULLY CONTROLLED OPERATION

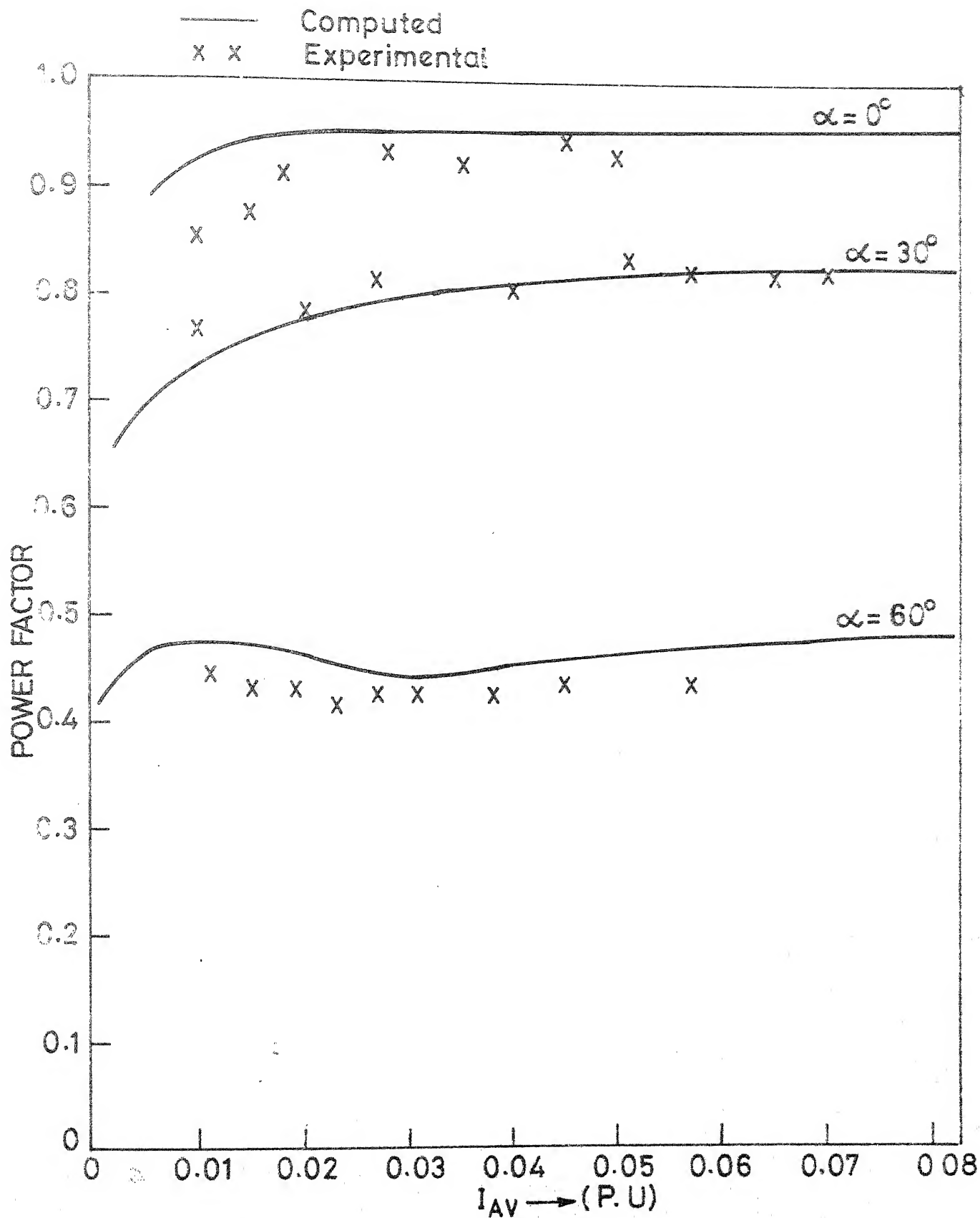


FIG. 4.5 EXPERIMENTAL VERIFICATION FOR FULLY CONTROLLED OPERATION

CONCLUSIONS

The modes of operation identified, for half and fully controlled three phase converted-fed d.c. separately excited motor, is used to analyse the drive accurately. With the help of these modes of operation the speed-torque characteristic of the drive and the armature ripple content is calculated. The power factor distortion-factor and the different harmonic contents in the source current are also calculated. Using these, we can predict the performance of any three-phase converter-fed d.c. separately excited motor.

The method described here for the calculation of filter inductance which eliminates discontinuous conduction and keeps the ripple within permissible limits can be used either for fully controlled or half controlled operation. The monograms can be used for any motor as they are given in normalised variables. This method eliminates discontinuous conduction and reduces ripple to prescribed value with minimum adverse effect on transient response.

REFERENCES

1. P. Mehta and S. Mukhopadhyay, "Modes of Operation in Converter Controlled d.c. drives", Proc. IEE, Vol. 121, No. 3, pp. 179-183, March 1974.
2. V. Subbiah and S. Palanichamy, "Investigations on Operation of Fully Controlled Thyristor Converters", Proc. IEE, Vol. 125, No. 1, pp. 58-59, Jan. 1978.
3. V. Subbiah and S. Palanichamy, "Mode Identification and Minimum Inductance Estimation for Fully Controlled Thyristor Converters", IEEE Trans. on IECI, Vol. IECI-20, No. 1, pp. 48-50, Feb. 1979.
4. G.K. Dubey, "Calculation of Filter Inductance for Chopper-Fed DC Separately Excited Motor", Proc. IEEE, Vol. 66, No. 12, pp. 1671-73, Dec. 1978.
5. P.B. Anjeneyulu, "Studies on Converter-Fed DC Drives", M.Tech. Thesis, IIT Kanpur, July 1979.
6. S.B. Dewan and A. Straughen, Power Semiconductor Circuits, John-Wiley and Sons, 1975.
7. SCR Manual, New York, GEC 1967.
8. Gottfried Moltgen, Line Commutated Thyristor Converters, Pitman, 1972.
9. H. Rissik and J.M. Donaldson, Mercury-Arc Current Converters, Pitman, 1960.
10. B. Ilango, R. Krishnan, R. Subramanian and S. Sadasivam, "Firing Circuit for three-phase thyristor bridge rectifier", IEEE Trans. IECI-25, Feb. 1978, pp. 45-49.
11. Remy Simard and V. Rajagopalan, "Economical Equidistant pulse firing scheme for thyristorised d.c. drives", IEEE Trans. IECI-22, pp. 425-29, Aug. 1975.
12. J.S. Wade, Jr., and L.G. Aya, "Design for Simultaneous Pulse Triggering of SCRs in three-phase bridge configuration", IEEE Trans. IECI-18, pp. 104-06, Aug. 1971.
13. R. Arockiasamy and S. Doraipandy, "A Novel Scheme to obtain voltage controlled time delay suitable for thyristor control", IEEE Trans. on IECI, pp. 29, Feb. 1976.
14. Hoang Le-Huy, "A digitally controlled thyristor trigger circuit", Proc. IEEE, pp. 89-90, Jan. 1978.

APPENDIX

Motor Specifications: 2.2 KW
220V armature voltage
220V shunt field excitation
11.6 A armature current
1500 rpm
1.94 ohms, armature resistance
17.5 mH, armature inductance